Jyrki Ristimäki

Sampling and Measurement Methods for Diesel Exhaust Aerosol

Jyrki Ristimäki

Sampling and Measurement Methods for Diesel Exhaust Aerosol

Thesis for the degree of Doctor of Technology to be presented with due permission for public examination and criticism in Sähkötalo Building, Auditorium S3, at Tampere University of Technology, on the 5th of December 2006, at 12 noon.

Abstract

Awareness of adverse health effects of urban aerosols has increased general interest in aerosol sources. As diesel engines are one significant urban anthropogenic particle source, diesel aerosols have been under intense research during the last decades. This thesis discusses the measurement issues related to the diesel exhaust particles, focusing on the effective density measurement with ELPI-SMPS and TDMA-ELPI methods and presents some additional performance issues not discussed in the papers.

As the emergence of volatile nanoparticles in the diesel exhaust is sensitive to prevailing circumstances there is a need to properly control the dilution parameters in laboratory measurements in order to obtain repeatable and reproducible results. In addition to the dilution parameters, the effect of ambient temperature on the light duty vehicle exhaust particulate emission was studied. It was found that turbocharged diesel engines were relatively insensitive to changes in ambient temperature whereas particle emissions from naturally aspirated gasoline vehicles were significantly increased at low temperatures.

The measurement of effective density and mass of aerosol particles with DMA and impactor was studied and applied to characterisation of diesel exhaust particles. The TDMA-ELPI method was used for determination of the volatile mass of diesel exhaust particles as a function of particle size. Based on the measurement results, condensation was suggested to be the main phenomena driving volatile mass transfer to the exhaust particles. Identification of the process and the separation of volatile and solid mass may become important as some health effect studies suggest the volatile fraction to be a key component causing the biological effects of diesel exhaust particles.

II

Preface

This work has been carried out in the Aerosol Physics Laboratory of the Institute of Physics at Tampere University of Technology in research projects funded by Ford Motor Company, European Union and Tekes.

I am grateful to my supervisor professor Jorma Keskinen for recruiting me to the aerosol laboratory and offering an opportunity to work in a field where several interesting topics such as motor vehicles, physics and environmental aspects are combined. I would also like to express my gratitude to all people in Aerosol Physics group for all the help in the projects. Especially I would like to thank Dr. Marko Marjamäki and Dr. Annele Virtanen for all the guidance concerning ELPI and co-operation in the development of effective density calculation. Thanks for all the co-authors for their contribution, above all to Dr. Matti Maricq for getting me on the track of writing articles.

Terhi, Jaana and Jaakko – thank you for keeping me busy at home so I did not have much time to worry about the thesis. Building a snowman or playing with Legos is much more important at home than writing thesis.

Jyrki Ristimäki

List of publications

I. Mathis U., Ristimäki J., Mohr M., Keskinen J., Ntziachristos L., Samaras Z., Mikkanen P. (2004) Sampling Conditions for the Measurement of Nucleation Mode Particles in the Exhaust of a Diesel Vehicle. *Aerosol Science and Technology 38* 12:1149-1160

II. Ristimäki J., Keskinen J., Virtanen A., Maricq M., Aakko P. (2005) Cold Temperature PM Emissions Measurement: Method Evaluation and Application to Light Duty Vehicles. *Environmental Science & Technology 39* 24:9424-9430

III. Ristimäki J., Virtanen A., Marjamäki M., Rostedt A., Keskinen J. (2002) On-line measurement of size distribution and effective density of submicron aerosol particles. *Journal of Aerosol Science 33* 11:1541-1557

IV. Virtanen A., Ristimäki J., Keskinen J. (2004) Method for Measuring Effective Density and Fractal Dimension of Aerosol Agglomerates. *Aerosol Science and Technology 38* 5:437-446

V. Ristimäki J., Keskinen J. (2006) Mass Measurement of Non-Spherical Particles: TDMA-ELPI Setup and Performance Tests. *Aerosol Science and Technology 40* 11:997-1001

VI. Ristimäki J., Vaaraslahti K., Lappi M., Keskinen J. (2006) Hydrocarbon Condensation in Heavy-Duty Diesel Exhaust. Submitted to *Environmental Science & Technology*

Other work related to the topic that the author contributed but not included in the thesis:

1) Virtanen A., Ristimäki J., Marjamäki M., Vaaraslahti K., Keskinen J., Lappi M. (2002) Effective Density of Diesel Exhaust Particles as a Function of Size. *SAE Technical Paper Series* 2002-01-0056

2) Ntziachristos L., Giechaskiel B., Ristimäki J., Keskinen J. (2004) Use of a Corona Charger for the Characterisation of Automotive Exhaust Aerosol. *Journal of Aerosol Science 35* 8:943-963

3) Virtanen A., Ristimäki J., Vaaraslahti K., Keskinen J. (2004) Effect of Engine Load on Diesel Soot Particles. *Environmental Science & Technology 38* 9:2551-2556

Contents

Nomenclature

Abbreviations

APM	Aerosol Particle Mass Spectrometer
C28	Hydrocarbon alkane with 28 carbon atoms
CPC	Condensation Particle Counter
CVS	Constant Volume Sampler
CMD	Count Median Diameter
DMA	Differential Mobility Analyzer
DMM	Dekati Mass Monitor
DOS	Di-Octyl-Sebacate
EEPS	Engine Exhaust Particle Sizer
ELPI	Electrical Low Pressure Impactor
FMPS	Fast Mobility Particle Sizer
GA	Genetic algorithm
GSD	Geometric Standard Deviation
NIST	National Institute of Standards and Technology
PM	Particulate Matter
PMP	Particulate Measurement Program
PP	Primary particle
RMS	Root Mean Square
SMPS	Scanning Mobility Particle Spectrometer
TDMA	Tandem Differential Mobility Analyzer
TEOM	Tapered Element Microbalance
TSP	Total Suspended Particulate

Symbols

η = viscosity

ρ = density

χ = dynamic shape factor

B = mechanical mobility

C = slip correction factor

F = force

V = volume

d = diameter of the particle

df = fractal dimension

g = gravity

m = mass

v = velocity

Subscripts

0 = unit value ($1000 kg/m^3$)

$aero$ = aerodynamic

$cond$ = condensation

eff = effective

$grav$ = gravity

mob = mobility

p = particle bulk value

ref = reference point

$Mass$ = mass equivalent particle

$True$ = true particle

X

1 Introduction

Air pollution has irritated people for centuries. Philosophers have made notes about poor air quality of Rome already A.D. 61[1] and the emergence of air pollution regulations date back to 1272 when King Edward I of England banned the use of sea coal in London[2]. As cities grew larger the smoke and air pollution problems became worse: In the 19th century Great Britain several committees studied the problem and police was empowered to enforce provisions against smoke[1]. Technological advancement did not always improve air quality; as the steam locomotive was invented and railroad travel started to flourish the smoke problem got even worse. Retrospective analyses of vital records from the end of the 19th century have implied smoke related deaths in London[2]. Some technological inventions also helped to decrease smoke problem. At the end of the 19th century a Frenchman Maximillian Ringelmann invented a kind of opacimeter, initially intended to tune up coal fired boilers, was later applied also for regulative purposes: E.g. in Philadelphia 1904 Ringelmann type opacimeter was used to classify smoke emissions and it was unlawful to emit too dark smoke[3]. With the help of technological improvements, such as use of electrical motor instead of steam engine together with the use of oil instead of coal, ash emissions decreased from its peak between years 1930-1950[1,4].

As the number of automobiles increased in the 20th century, new air pollution problem was to emerge: Los Angeles experienced its first smog event in 1943 that could not be explained by traditional sources. Hydrocarbon emissions were found to play a role in formation of this new type of smog[*,5]. In unfavourable

---

[*] First used by Dr. Henry Antoine Des Voeux 1905 in his paper "Fog and Smoke"

weather conditions the exhaust emission from motor vehicles can form large, light scattering particles through photochemical reactions[5]. To improve outdoor air quality, regulations were set for several different aerosol sources including motor vehicles. Before 1970 regulations concerned gaseous components like volatile organic compounds, nitrogenous oxides and carbon monoxide[6,7]. The first regulation directly related to aerosol particles was effective in 1970 in the form of exhaust opacity. Opacity remained as the only particle related regulation until 1987 when particulate matter (PM) mass from motor vehicles were federally regulated in the USA. In Europe the first mass based emission standards EURO I were introduced and effective in 1992 and 1994 respectively. Since then the mass emission limits have decreased significantly. The EURO IV (2005) limits for the allowed PM are over 80% and 90% lower than the EURO I levels for light and heavy duty diesel vehicles respectively. The decrease in PM emission has its implications also to the PM measurement at the future emission levels. One difficulty is the volatile hydrocarbons, which may be adsorbed on the filter and cause sensitivity and repeatability problems for the traditional filter mass measurement[8].

The driving force to limit the exhaust PM mass emissions have been the risen awareness of the adverse health effects of ambient PM[9]. In 1971 regulations concerning ambient PM mass, were introduced in the USA[10]. This was rather late considering that studies suggesting PM as a factor causing the adverse health effects date back to the 1931[11,12]. Nowadays, PM has been estimated to cause nearly 100000 pre-mature deaths in Europe alone every year[13]. Since the introduction, the outdoor PM mass limits have shifted from regulating the total suspended particulate (TSP) to mass of particles having aerodynamic diameter smaller than 10µm (PM_{10}). Currently regulations for particles smaller than 2.5µm in aerodynamic diameter ($PM_{2.5}$), are put to effective in USA[14] and

2

Europe[15] as these particles can penetrate deep into the lungs[16,17]. However, as the origin of the adverse health effects remains unveiled, more information is needed on the properties of the urban ambient particles. As particle emissions from internal combustion engines are one major source of urban PM, its properties have been under intense research – within and outside automotive industry.

This thesis has been motivated by general interest in aerosols, measurements and motor vehicles. The two targets of this thesis were: 1) Study the measurement of internal combustion engine exhaust particles (Papers I and II) 2) Study the measurement of effective density and mass of aerosol particles (Papers III, IV, V and VI). In the first paper a dilution concept designed for repeatable and reproducible measurement of volatile diesel nanoparticles was studied. The second paper studies how the emission from different engine technologies and the instrument response, is affected by change in the ambient temperature. Both of these papers indicate difficulties in reproducible measurement of the volatile nanoparticle emission. In paper III a methodology to measure average effective density for particle distribution is presented. Paper IV is an extension to the paper III in order to make the method more applicable to the measurement of diesel exhaust particles. Paper V utilises the numerical calculation method presented in paper III in another common measurement setup and presents the performance of the combined system. In paper VI the methodology, presented in paper V, is used to study the volatile mass fraction of diesel exhaust particles.

The paper I is based on measurements, carried out by author and Dr. Urs Mathis. The results are also presented in author's M.Sc. thesis. The data analysis and major fraction of writing of the papers II, V, and VI has been done by

author. All the measurements in the papers V and VI, and some of the measurements in paper III are made by author. Author is also responsible for the Matlab code used to calculate the effective densities in papers III-VI.

2 Particulate emission measurement from vehicles

Though there is no common real life driving pattern, a standardized driving pattern is needed to make the laboratory measurements repeatable and reproducible. In practice two approaches has been used: 1) Measure several steady state load points and define emission as some kind of average of the load points. 2) Drive a standardized driving cycle with strict speed limits and define the emission over the cycle. The first method is followed with heavy duty and the latter with light duty vehicles. Examples of the driving cycles for the light duty vehicles are presented in Figure 1.

Regardless of differences in the driving cycles (Figure 1), actual regulatory limits and other detailed specifications, different emission particulate standards are similar: A driving pattern is driven and exhaust PM is collected on a filter. The filter is weighted and mass emission is calculated. As the regulative limits for the PM has significantly decreased the emitted mass, repeatability problems with the standard filter measurement starts to emerge; gaseous hydrocarbons adsorbed on the filter begins to count in the mass measurement with the forthcoming emission limits[8]. To overcome the repeatability issues the effects of several sampling details such as filter temperature and face velocities, are considered[18,19].

4
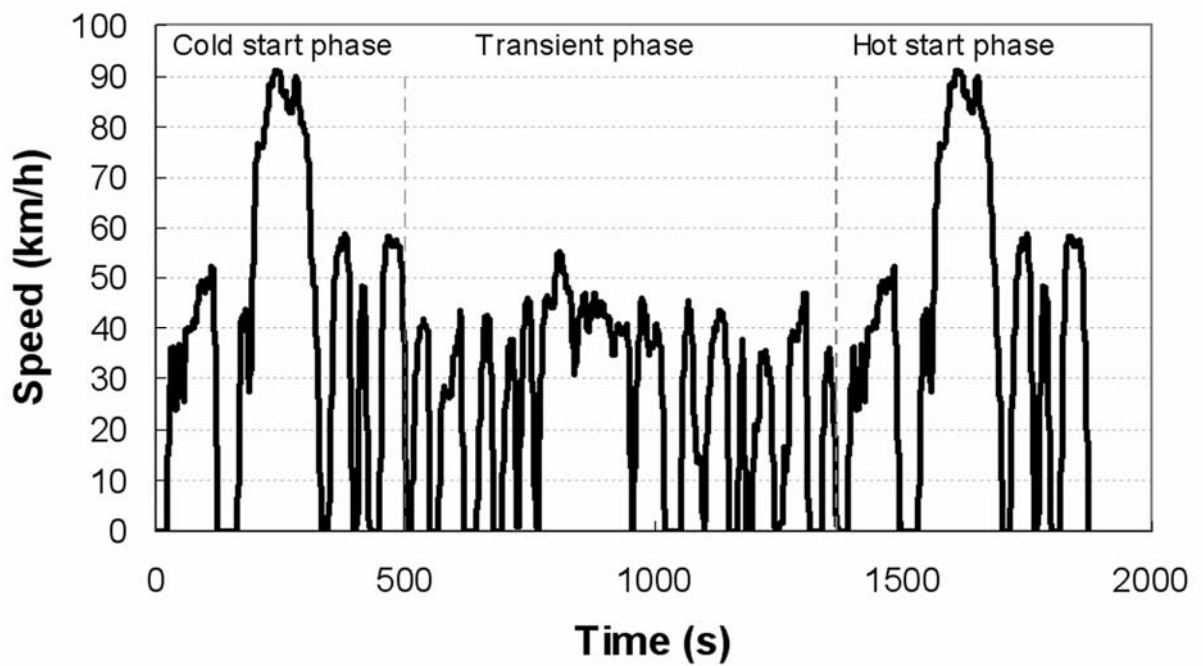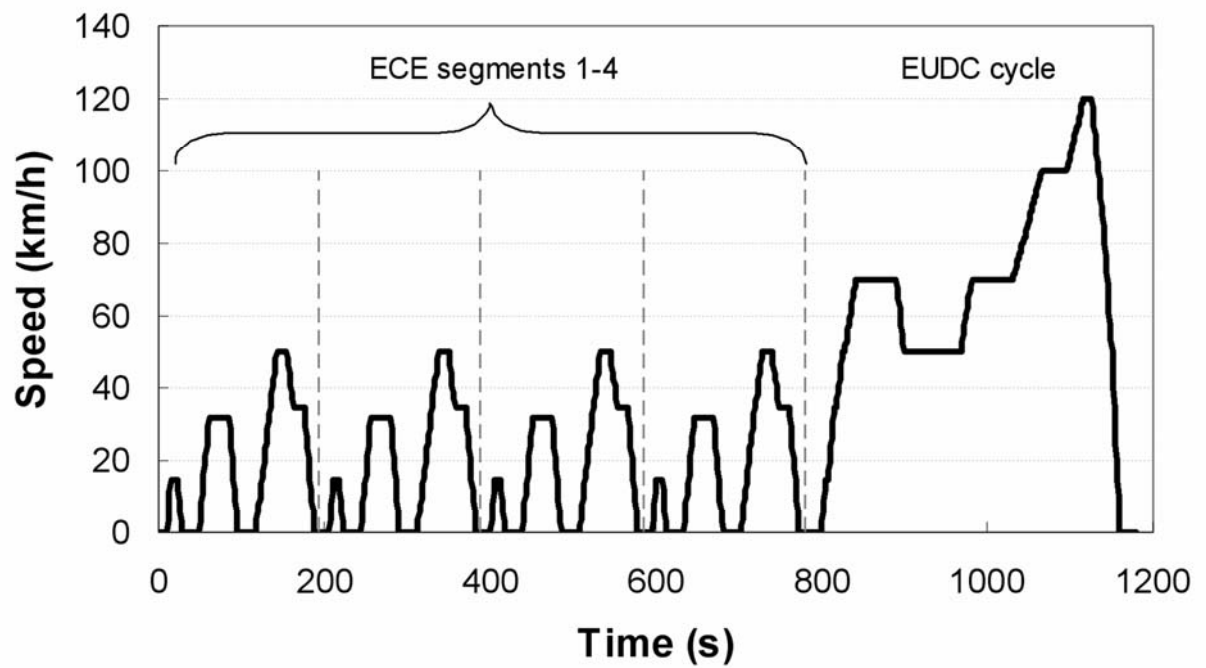
Figure 1 Driving cycles for light duty vehicles. European ECE+EUDC cycle (above) and American FTP-75 cycle (below).

2.1 Effects of sampling on exhaust particles

Incomplete combustion and lubricant leaks result in an escape of carbonaceous soot particles and hydrocarbons from the cylinder. Initially the number of the primary soot particles is large enough for fast coagulation and formation of larger particles[20,21]. These larger particles are called agglomerates (Figure 2). When present, hydrocarbons can be adsorbed on the surface of the soot particles (Figure 2). While the hot exhaust gas cools, some of the gaseous components may also condense on the particles. If the exhaust cools fast enough, condensation is unable to remove the excess material from the gas phase and new volatile particles can be formed from the gaseous components by nucleation[22,23,24] (Figure 2). Such a rapid cooling can occur e.g. when the exhaust gas enters the atmosphere or a dilutor. Properties of the gaseous compounds and rate of temperature change define which of the processes take place and how the volatile mass is distributed on the particles. In all, over 50% of the measured particulate mass can be volatile[25,26]. As the formation of the nucleation mode particles is sensitive to kinetics and several other dilution parameters[23,24,27] (Paper I), reproducible measurement of the volatile matter or particles is difficult.
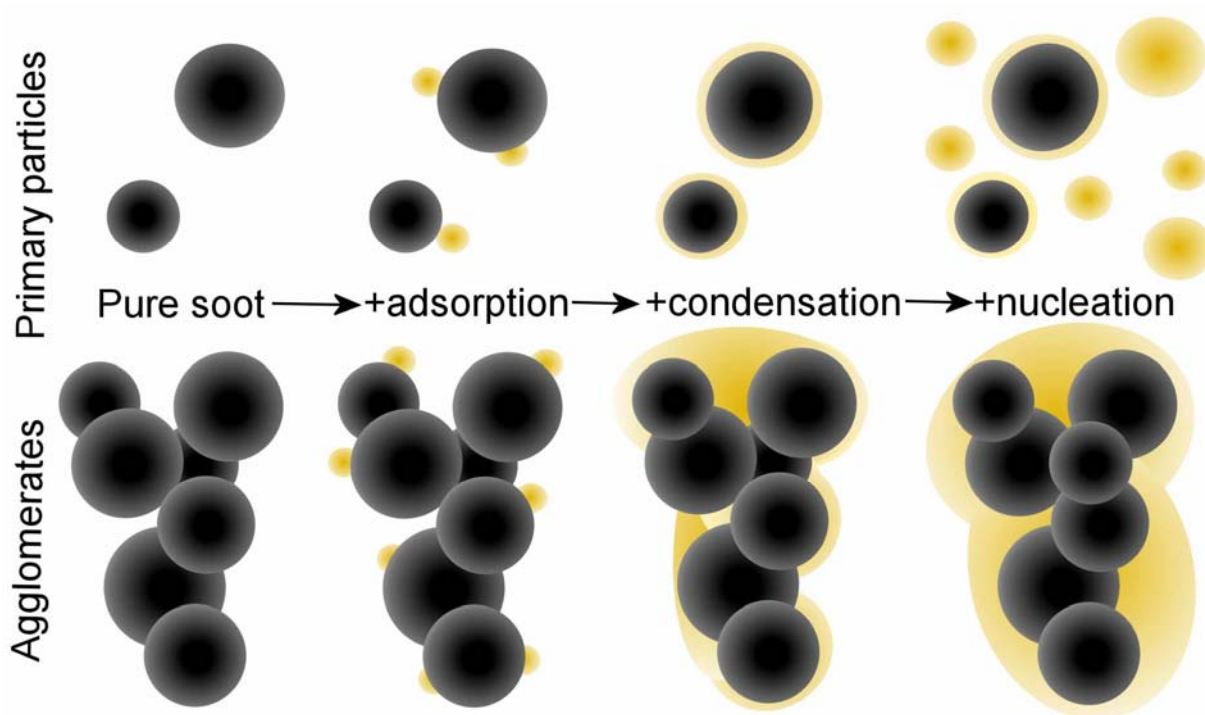
Figure 2 Schematic figure of the diesel soot particles, mass transfer of volatile compounds on the particles.

In the Particulates[*] program new vehicle exhaust dilution scheme was developed in order to establish a method for reproducible measurement of solid and volatile particles[28]. The partial flow dilution strategy was selected as it enables easier control over the dilution parameters than normal full flow constant volume sampler (CVS). Paper I covers several experimental issues regarding nucleation mode formation in order to establish a set of dilution parameters for the basis of good reproducibility of nucleation mode. A new finding presented in paper I was that the formation of the nucleation mode particles can be suppressed by increasing the airspeed used to cool the engine. It

---

[*] Characterisation of exhaust particulate emissions from road vehicles ; Funded by the European commission – Directorate General Energy and Transport (EC-DG TREN)

was verified that the suppression of the formation of nucleation mode particles was related to exhaust pipe cooling. This finding demonstrates the sensitivity of nucleation mode particle formation and extends the need for proper parameter control outside the actual dilution process. In the worst case it ruins the reproducibility of the nucleation mode in dynamometer measurements as the (air) flow pattern around the exhaust pipe can depend on the number of dynamometer rolls. Other authors have also demonstrated the suppressing effect of exhaust pipe cooling on formation of nucleation mode particles[29]. In general, this finding is related to the storage release effects[30,31]. As a continuation of the work done in paper I, Ntziachristos et al[32] reported inter-laboratory results of the repeatability and reproducibility with the dilution parameters suggested in paper I.

In CVS, used to dilute the exhaust gas for the regulatory purposes, a constant flow is maintained in the dilution tunnel. A drawback of such arrangement is that the dilution ratio changes with the exhaust gas flow: When the exhaust flow increases, the dilution ratio decreases. Therefore, during the test cycle, the conditions for the volatile matter behaviour can change from adsorption to nucleation. In turn this can hamper repeatability and reproducibility of filter PM mass measurements as some of the previously collected volatile material may also evaporate from the filter and dilution tunnel walls. Though the repeatability and reproducibility may suffer from the variable dilution ratio of the CVS, the non-constant dilution ratio may simulate random dilution conditions of the real world.

2.2 Aspects to the future PM measurement

The lack of concentration standard for aerosol measurements makes it difficult to select an alternative for the mass measurement for regulatory purposes. In addition, as no typical shape of aerosol particle exists, aerosol measurements except number count and mass, are measurement of some equivalent value: mobility, electrical mobility, aerodynamic or optical diameter etc. This means that in the instruments, the response of the true, possibly non-spherical particle is compared to the response of a spherical calibration particle.

Considering only spherical particles, the best aerosol calibration standard is for diameter. The diameter of commercially available polymer microspheres can be traced back to National Institute of Standards and Technology (NIST). In practice, however, as aerosols are dynamic systems, one must be careful when generating aerosol from such microspheres. Too high concentration either in the suspension or in the gas phase may result in the coagulation of the spheres. In turn this changes concentration and the equivalent diameter. Additional difficulties in calibration and aerosol generation rise from the fact that aerosols exists over several orders of magnitude in diameter. In practice, aerosol particles of specific (equivalent electrical mobility) diameter are generated from aerosol distribution with the help of Differential Mobility Analyzer (DMA)[33,34].

The lack of calibration standards poses a challenge for measurement of absolute values from aerosols. Considering future PM emission limits, if some other parameter than mass would be accepted for the measured exhaust PM characteristic, more sensitive methods can be found[35]. Unfortunately from the regulative point of view, the more sensitive methods do not necessary relate to any common property. On the other hand, this may be the case also with the adverse health effects.

One candidate for future PM measurement setup, reaching for better sensitivity, is currently developed in the Particulate Measurement Program[*] (PMP). In the PMP project a common full flow dilution system is used and in addition to normal mass measurement the total number concentration of thermally treated (solid) particles is measured with a Condensation Particle Counter (CPC)[36]. First reports imply smaller variation in number based results than obtained with refined filter mass measurements[37]. As in the PMP project the nucleation mode particles are suppressed with thermal treatment, the method does not suffer from the sensitivity of formation of the volatile nanoparticles.

## 2.2.1 PM emission and subzero ambient temperature

The negligence of the measurement of volatile nanoparticles is a drawback of the PMP setup as these particles do exist at the roadside[38,39]. Additionally, the amount of roadside nanoparticles is affected by the ambient temperature[39]. Therefore it is unfortunate that the PM emission at cold ambient temperatures is not controlled though the first regulations concerning low ambient temperature gaseous emissions were established in 1992 in the US[40]. In Europe, EU directive regulating gaseous emissions at -7°C was effective in 2002[41].

Paper II studied how the emission of current light duty vehicles is changed due to decrease in ambient temperature. The focus was on the measurement of diesel exhaust nucleation mode particles at sub-zero temperatures; especially the possibility of nucleation mode particle evaporation due to temperature rise in the instruments located at normal room temperature. This was done by

[*] Particle Measurement Programme ; Transport division of United Nations Economic Commission for Europe (UNECE); http://www.unece.org

10

simultaneous measurement of sub-zero diesel exhaust sample with two pairs of ELPI (Electrical Low Pressure impactor)[42,43] and SMPS (Scanning Mobility Particle Spectrometer)[44]. One instrument pair (ELPI and SMPS) was located at ambient temperature of the vehicle (sub-zero) and the other pair was located at normal room temperature (+24°C). Fortunately, no signs of evaporation of the nucleation mode particles were detected. The outcome of the paper II was that the instruments (ELPI and DMA) can be located at room temperature without distorting the number distribution at the sub-zero temperature. This simplifies the measurement setup in future sub-zero PM research studies. The number based emissions measured over the ECE+EUDC cycles are presented in Figure 3.
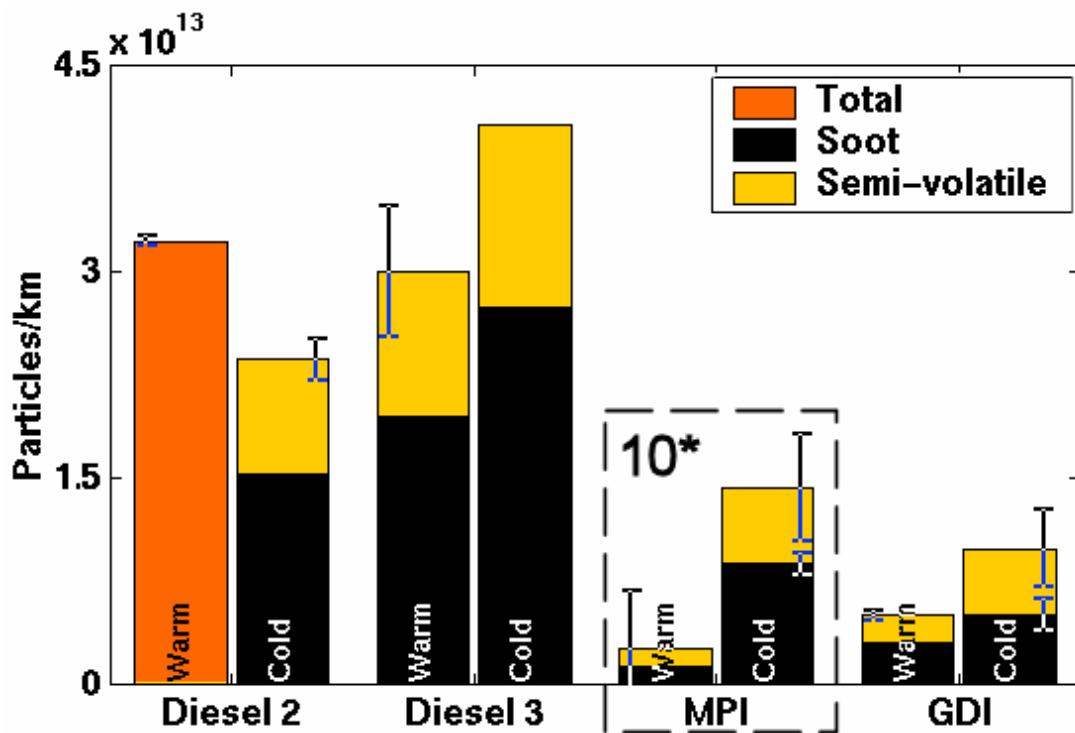
Figure 3 The average emission of particles (#/km) over the ECE+EUDC cycle. MPI refers to common (multiple port fuel injection) gasoline engine and GDI to gasoline direct injection technique. The MPI values are multiplied with 10 in order to make them visible on same y-axis. (Paper II)

It can be concluded from the Figure 3, that the particulate emissions from the turbocharged diesel engines are not as severely affected by the ambient temperature as the emission from the gasoline technologies. However, the PM emissions from the gasoline technologies are significantly lower than with the diesel technology at both ambient temperatures. The vehicles were not equipped with particulate filters.

Considering the measurement of the particle number, it should be noted that for each technology tested (Figure 3), about one third of the emitted particles were (semi-)volatile in nature. As these particles would not be measured with the measurement setup of the PMP project, disagreement between the real world and laboratory particulate number will occur. If it turns out that most of the future PM emissions are volatile[18] and the volatile diesel PM is the key component causing the adverse biological effects[45,46], the regulative measurement suggested by PMP program does not necessarily decrease the emission of harmful PM. In the worst case, if only number of solid particles, i.e. the surface available for condensation, is limited by regulative measures, the number of volatile particles may actually increase. This occurs e.g. with particulate filters[47,48,49].

2.2.2 Alternatives in diesel exhaust PM measurement

Mass could be regarded to be the most common and important property of aerosol regarding the exhaust PM as the regulations are based on total mass. Though the filter method faces sensitivity problems, other (electrical) mass measurement methods have also their limitations: Accurate, "single" particle mass measurement techniques, such as Millikan cell[50], Aerosol Particle Mass

Spectrometer[51] (APM) or special arrangement of Tandem-DMA[52] (TDMA) are not suitable for measuring total PM over transient cycle. The real time (direct) total mass measurement techniques, such as piezoelectric crystal method or tapered element oscillating microbalance (TEOM)[53] also suffers similar sensitivity problems at new mass emission limit levels as standard filter mass measurement[8,19,54].

Particles could be measured with devices such as Photoelectric/Diffusion Chargers or CPCs. However, though these instruments are based on measurement of electrical charge or particle count and have higher sensitivity than mass based methods[35], the problem is that their response is not directly related to the regulated mass. Instead, many of the instruments (Dekati Mass Monitor (DMM)[55,56], ELPI , Engine Exhaust Particle Sizer (EEPS) or Fast Mobility Particle Sizer (FMPS) and SMPS, utilizing the effective density concept to calculate the total mass, have been found to correlate well with normal filter based method[19].

3 Effective density concept and single particle mass

The effective density concept links the mobility diameter to the aerodynamic diameter. Previous studies[57,58] have shown that with the help of effective density and mobility diameter the particle mass can be calculated regardless of its shape. In following the main equations establishing the link between aerodynamic and mobility diameters and the effective density concept are presented.

The dynamic shape factor is defined as the ratio of the true drag (F_{true}), experienced by the particle, to the drag experienced by the mass equivalent sphere (F_{mass}) at the same speed (Equation 1)[58,59].

Equation 1
$$\chi = \frac{F_{true}}{F_{mass}}$$

As the mechanical mobility (B) of two particles are same if they have the same terminal velocity (v) in a force field ($v=FB$) a relationship between mass (d_{mass}) and mobility equivalent diameter (d_{mob}) can be constructed.

Equation 2
$$F_{true} = \chi F_{mass}$$

Equation 3
$$\frac{v}{B_{true}} = \chi \frac{v}{B_{mass}}$$

Equation 4
$$\frac{1}{B_{true}} = \frac{\chi}{B_{mass}} = \frac{1}{B_{mob}}$$

By using the definition for mechanical mobility we obtain

Equation 5
$$\chi \frac{3\pi\eta d_{mass}}{C_{mass}} = \frac{3\pi\eta d_{mob}}{C_{mob}}$$

Equation 6
$$d_{mass} = \frac{C_{mass}}{\chi C_{mob}} d_{mob}$$

14

"*C*" refers to the slip correction factor, "ρ" to density and "η" to viscosity. The subscripts "*mob*" refer to mobility and "*mass*" to mass equivalent particle.

Aerodynamic diameter is considered as the diameter of a spherical particle having unit density (1g/cm^3) and the same settling velocity as the true particle. Relationship between aerodynamic and mass equivalent diameter can be obtained from their definitions: By the definition of aerodynamic diameter, both particles have the same settling velocity in the gravitational field:

Equation 7
$$\upsilon = F_{grav} B_{true} = F_{grav} \frac{B_{mass}}{\chi} = F_{grav\_aero} B_{aero}$$

Equation 8
$$\frac{\pi \rho_p d^3_{mass}}{6} g \frac{C_{mass}}{3\pi\eta d_{mass} \chi} = \frac{\pi \rho_0 d^3_{aero}}{6} g \frac{C_{aero}}{3\pi\eta d_{aero}}$$

g refers to gravity and subscripts "*aero*" to aerodynamic, "*p*" to particle bulk value and "*0*" to unit value (1g/cm^3).

After rearrangement we end up with Equation 9.

Equation 9
$$\rho_p d^2_{mass} = \chi \frac{C_{aero}}{C_{mass}} \rho_0 d^2_{aero}$$

Using Equation 6 we obtain:

Equation 10
$$\frac{C^2_{mass}}{\chi^2 C^2_{mob}} \rho_p d^2_{mob} = \chi \frac{C_{aero}}{C_{mass}} \rho_0 d^2_{aero}$$

Finally after rearranging, we get

Equation 11
$$\rho_0 C_{aero} d_{aero}^2 = \left[\frac{C_{mass}^3}{\chi^3 C_{mob}^3} \rho_p \right] C_{mob} d_{mob}^2 = \rho_{eff} C_{mob} d_{mob}^2$$

Where effective density (ρ_{eff}) is defined as:

Equation 12
$$\rho_{eff} = \left(\frac{C_{mass}}{\chi C_{mob}} \right)^3 \rho_p = \frac{C_{aero} d_{aero}^2}{C_{mob} d_{mob}^2} \rho_0$$

Using Equation 10 particle mass can be obtained with the help of mobility diameter and effective density.

Equation 13
$$m_{true} = \rho_p \frac{\pi d_{mass}^3}{6} = \rho_p \frac{\pi}{6} \left(\frac{C_{mass}}{\chi C_{mob}} \right)^3 d_{mob}^3 = \frac{\pi}{6} \rho_{eff} d_{mob}^3$$

By rearranging we can define the effective density as the true mass divided by the volume of mobility equivalent particle.

Equation 14
$$\rho_{eff} = \frac{m_{true}}{\frac{\pi}{6} d_{mob}^3}$$

As the aerodynamic diameter is an equivalent diameter, the changes in the mobility and aerodynamic diameter are not necessary similar. E.g. if light substance (e.g. Di-Octyl-Sebacate (DOS)) start to condense on heavy spherical particle (e.g. silver), the aerodynamic diameter starts to decrease though the mobility diameter and mass is increased.

3.1 Morphology, condensation and effective density

As the larger diesel exhaust particles are formed from the smaller primary particles through a random collision process, there is no typical shape for agglomerate particle. However, there is a relation between particle mobility and mass[60,61]. Additionally, as the effective density can be regarded as the ratio of mass to mobility equivalent particle volume (Equation 14) the fractal dimension (*df*), used to describe the ratio of mass to radius of gyration[62], can also be used to describe the behaviour of the effective density as a function of particle size (Equation 15). This concept has also been used with diesel exhaust particles[63].

Equation 15
$$\log_{10}\left(\rho_{eff}\right) = -(3 - df)\log_{10}\left(\frac{d_{mob}}{d_{ref}}\right) + \log_{10}\left(\rho_{ref}\right)$$

In Equation 15 the ρ_{ref} and d_{ref} are the effective density and mobility diameter at a reference point respectively. The smaller the fractal dimension the faster the effective density decreases as the particle mobility size increases. Value 3 for fractal dimension corresponds to constant density. For diesel particles the 1.8g/cm^3 has been measured for the bulk material density[64]. 1.8g/cm^3 can be regarded as the reference value (ρ_{ref}) in Equation 15. The corresponding mobility diameter (d_{ref}) value can be selected to the primary particle size. Based on electron microscope analysis, this was estimated to be 18nm (Paper VI). Relatively typical value for the fractal dimension of diesel exhaust particles is ~2.3, though reported values range from 2-3[63,65]. One possible explanation for the broad range of fractal dimension values is condensation.

As the condensing hydrocarbons are rather large, they have small diffusion coefficient. Therefore it is enough to consider condensation in continuum region where the condensation is related to the diameter of the particle. Combining with Equation 15, and assuming no change in particle mobility size, it can be

seen that due to condensation of hydrocarbons the effective density increases with decreasing particle size. In turn this leads to decrease in the fractal dimension.

Equation 16 $\quad \rho_{eff\_new} = \dfrac{m + m_{cond}}{V_{mob}} = \rho_{eff} + \dfrac{m_{cond}}{V_{mob}} \propto \rho_{eff} + \dfrac{d_{mob}}{V_{mob}} = \rho_{eff} + \dfrac{6}{\pi d_{mob}^2}$

4 Measurement of effective density

Equation 12 can be directly used for calculation of effective density when aerodynamic and mobility diameters are known. Fortunately these diameters can be obtained from common instruments. The mobility diameter can be obtained from the DMA and the aerodynamic diameter can be determined with an impactor. Traditionally the DMA is used to acquire monodisperse particles to calibrate the impactor[66,67,68]. Once the impactor has been calibrated with particles of known density, the collection efficiency curves can be used to determine the effective density of unknown particles[58,69,70,71,72]. In this traditional measurement setup the DMA and impactor are in series.

New approach, based on parallel setup of ELPI and SMPS, to determine effective density was introduced by Ahlvik, Ntziachristos, Keskinen and Virtanen[73] in 1998. The approach was based on comparison of number distributions measured by ELPI and SMPS. Unfortunately, there was a discrepancy between the effective densities obtained with parallel and serial methods. Additionally, in other studies, the effective density obtained from traditional DMA-impactor method increased the difference between ELPI and SMPS number distributions[74].

The discrepancy in the number distributions of ELPI and SMPS is partly caused by the simple inversion technique used in ELPI. This can be demonstrated by simulating the ELPI response to a known mobility distribution[75]. Fortunately, the non-idealities in the ELPI number distribution calculation can be avoided in the effective density calculation if the calculation of ELPI's number distribution is discarded.

4.1 Parallel method – calculation with impactor kernel

In the parallel ELPI-SMPS effective density method (Paper III and IV) the SMPS measured number distribution on mobility axis is converted to the ELPI measured current distribution on aerodynamic axis by using the charger efficiency curves[76], impactor kernel functions[77] and the effective density. The effective density resulting in the best fit between the measured and simulated ELPI currents is considered as the effective density of particles. As the method is based on simultaneous parallel measurement with ELPI and SMPS, it is nearly on-line in operation and the effective density can be obtained without any special arrangement of the instruments. More detailed description of the method is presented in paper III. As an extension to the constant density assumption, used in paper III, an approach with fractal density profile is presented in paper IV.

## 4.2 Performance of the parallel method

The performance of the parallel method was tested with several simulations and laboratory measurements in paper III. The simulations give insight to sensitivity and bias errors whereas laboratory experiments were necessary to obtain conception of the true performance of the method.

The simulation results in papers III and IV showed that the parallel method can cope with some noise in the measurements. In both papers noise was added to mobility (SMPS) distribution and ELPI currents before calculating the effective density. For constant density (paper III) the effect of 10% root mean square (RMS) noise in the measurements resulted in 4% variation in the calculated effective density. The average of the results was the input density.

In the paper IV, a 2 variable model, utilizing fractal concept for the effective density was utilized. One variable defines the effective density at the count median diameter (CMD) and the other variable defines fractal dimension. In these simulations, 5 and 10% RMS noise was added for SMPS and ELPI measurements respectively. The deviation of the variables was found to depend on the input fractal dimension. As the fractal dimension decreases, the width of aerodynamic distribution decreases and the number of ELPI impaction stages, where the particles are collected aerodynamically, decreases. Therefore the result is more affected by the noise as the fractal dimension decreases. If the fractal dimension is small enough (~1.8), large particles on the mobility axis are aerodynamically smaller than small particles with high effective density. In such cases the distribution is reversed on the aerodynamic axis.

The performance of the parallel method was tested also with laboratory measurements. Though the average error in the effective density of the laboratory experiments was relatively low, typically below 10%, a bias error was observed even with spherical particles e.g. in DOS measurements. All the measured densities for DOS particles were below the bulk value (Figure 7 in paper III) with the average error less than -6%. Large error values (~30%), especially for distributions with CMD close to 40nm, were obtained. These

errors were considered to originate from the errors in the impactor model, especially in the lowest impactor stages. New measurements with recently calibrated impactor unit imply significant improvement at small particle sizes (Figure 4). It should be noted that as the distributions have certain width it is possible to obtain information on the effective density for the distributions having CMD below the lowest cut-point of ELPI (~30nm) (Figure 4).
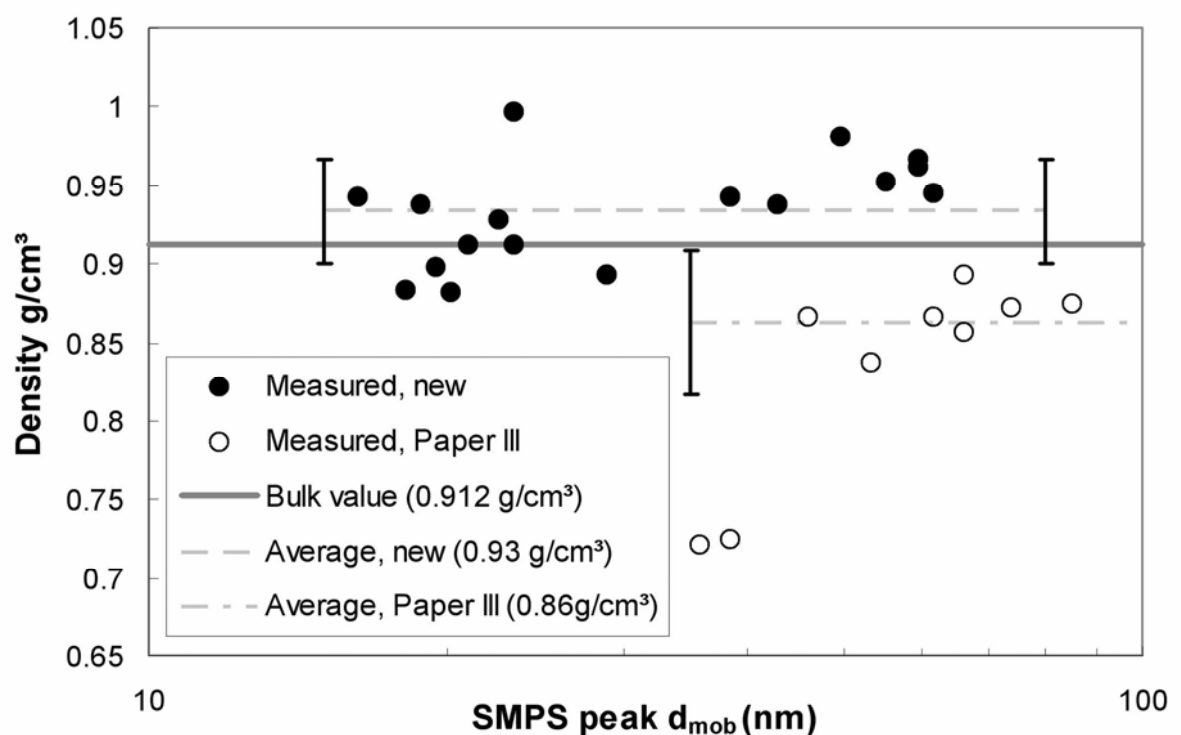
Figure 4 Comparison of old (paper III) and new measurement results for DOS particles below 100nm. Improvements in impactor model result in more accurate results.

However, as the impactor has been calibrated with DOS particles, the performance with DOS particles does not verify the impactor model correctness with particles of different effective density. In terms of average densities laboratory measurements with several different substances resulted with nice

agreement with material bulk densities. The difference was below 15% for all measured materials (Figure 5). This suggested that the impactor model is valid and method can be used for effective density measurements in general.
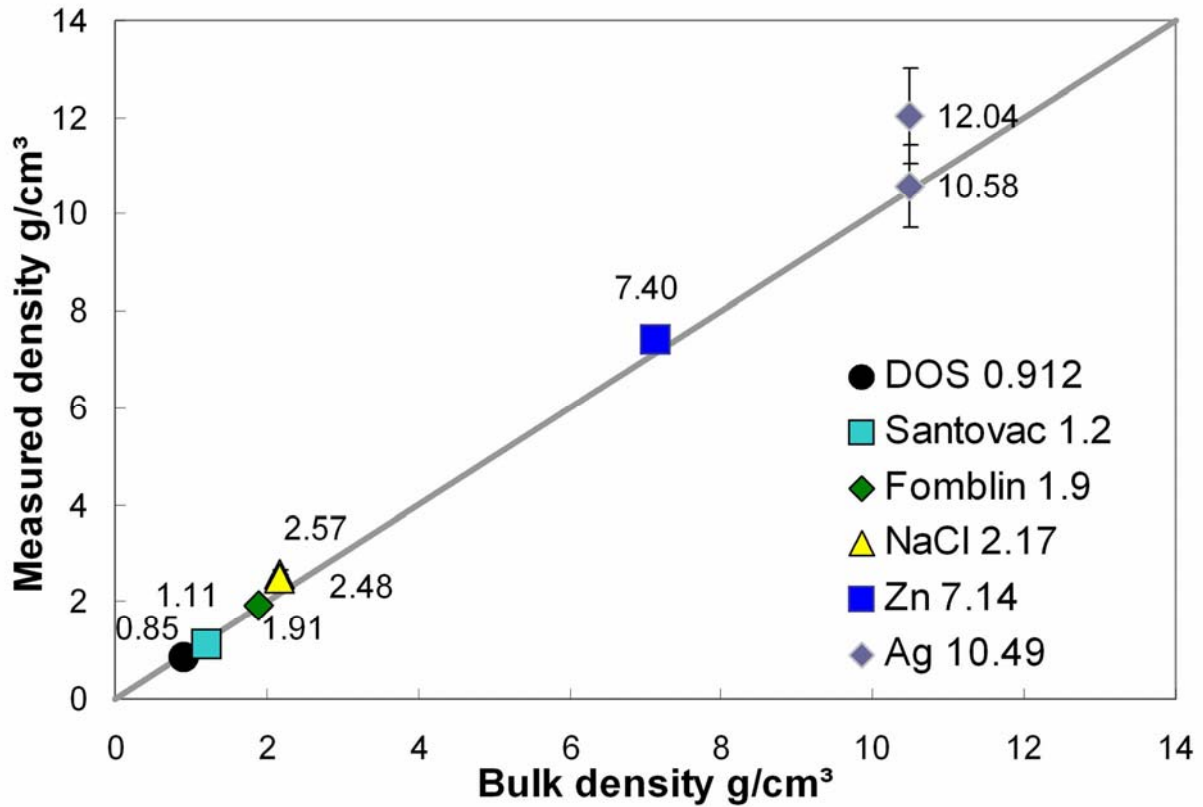
Figure 5 Comparison of measured effective density values with bulk densities. Data from paper III.

After the employment of the two variable method, presented in paper IV, there has been comparisons between the fractal dimension values of the effective density of diesel exhaust found with parallel method to the values obtained by other methods[78]. In general, the results with the parallel method have higher fractal dimension than obtained with the DMA-impactor or DMA-APM methods. Reason for this can be seen also with a simple simulation (Figure 6). Simulation reveals that parallel method gives the effective density profile close

to the CMD of the distribution[79] whereas with the serial method particles larger than CMD are usually measured. Therefore a different estimation for the slope is obtained. The input value for the fractal dimension at the right hand side of the distribution is lower than at the CMD. This is also verified in laboratory measuremens[79].
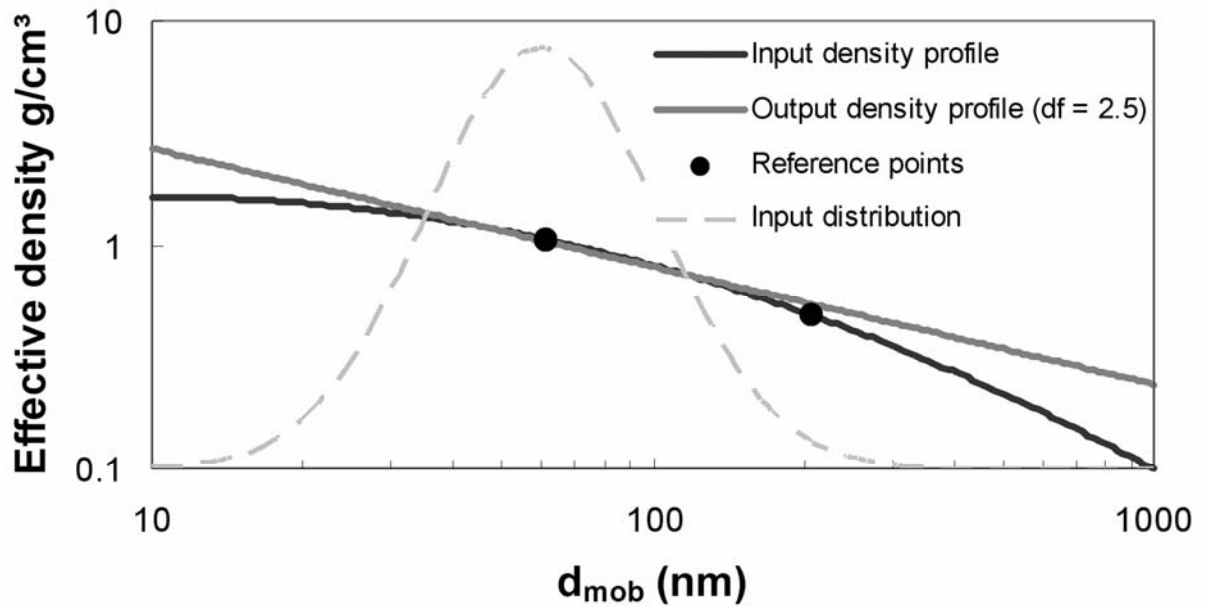
Figure 6 Simulation of ELPI-SMPS method response, with fractal density profile assumption, to non-constant-fractal input density. Steepness of the slope is given as value for fractal dimension (df) in two reference points. The ELPI-SMPS method gives the fractal dimension in the vicinity of the CMD. The dashed line in the background show the location and width of the diesel like number distribution.

The difference in ELPI currents with the two density profiles presented in Figure 6 is rather marginal as presented in Figure 7. Though there is rather large error percentages in some of the channels, the error percentages of the 3 highest currents are rather low. Additionally, as the relative fraction of current

outside the 3 highest channel values is low, even small errors in the calibration or noise can vitiate the search of true density profile.
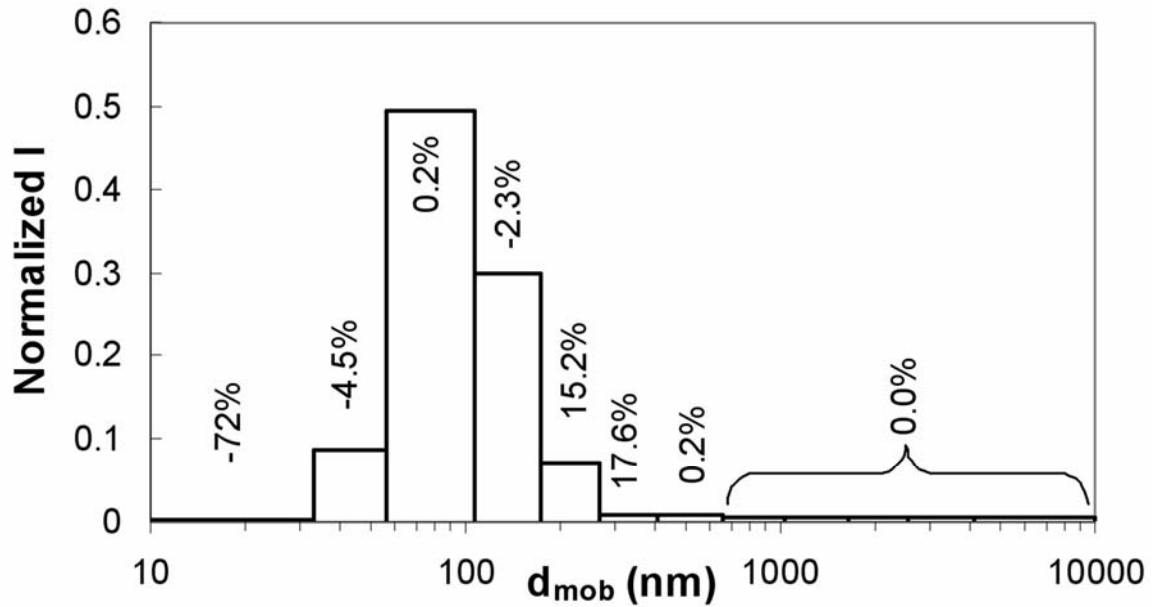

Figure 7 Normalized current distribution and percent difference between the simulated ELPI responses to the input distribution with the two density profiles presented in the Figure 6.

4.2.1 Effect of errors in the SMPS number distribution

As the parallel method gives density in the vicinity of the CMD, it can be concluded, and also verified with simulations, that deformation in the shape of the number distribution does not affect the result as long as the shape close to the CMD of distribution is correct. However, if the distribution is shifted on the mobility axis, the obtained effective density is affected. Example of this is presented in Figure 8 for 1 and 2 parameter density models. The error percentages in effective densities and the fractal dimension are presented as a function of the error in the CMD of the mobility distribution. The CMD and

24

GSD of the input distribution used in the simulation were 60nm and 1.7 respectively.
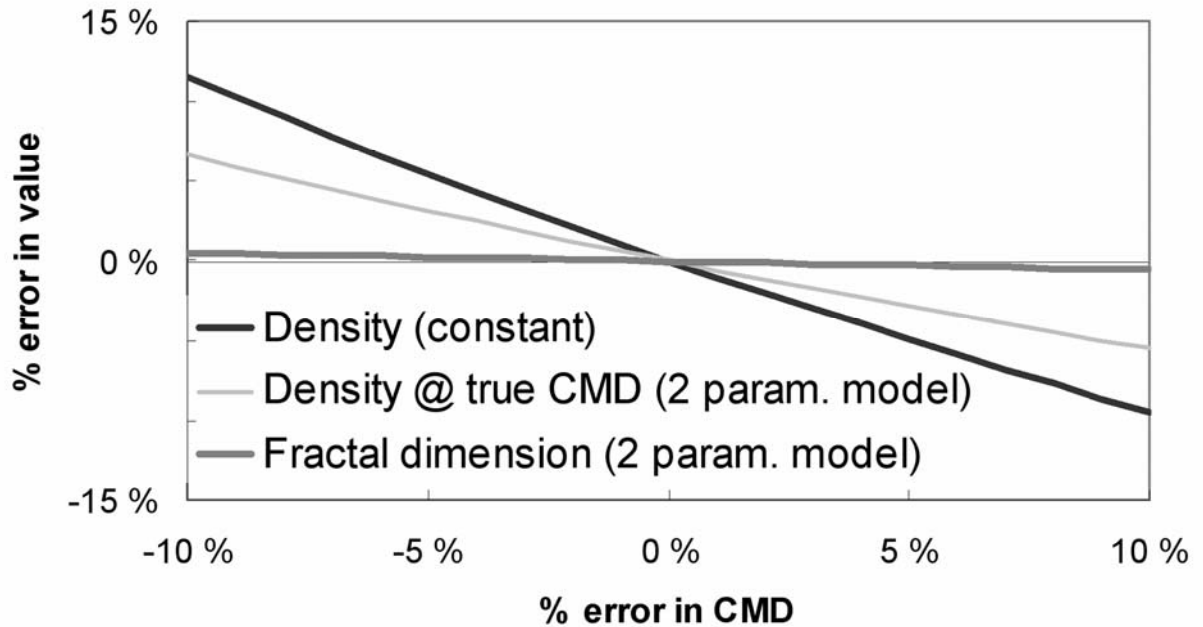

Figure 8 Error in the effective density and the fractal dimension as a function of error in the CMD with constant and 2 parameter models. The CMD and GSD of the input distribution were 60nm and 1.7 respectively.

4.2.2 Errors in the ELPI model

ELPI is usually calibrated with monodisperse particles obtained from DMA[43,67,80]. When calibration has been done slight deviation in the consecutive points exists[81]. Several explanations, such as noise, can be suggested. In addition to the random errors, greasing of the foils[82] and the amount of collected material[83] on the impaction plate, affect the collection characteristics of the stage. These may lead to some bias error in the effective density calculation.

Perhaps the most difficult errors in the ELPI calibration are the bias errors as the noise errors can be overcome by measuring more calibration points. In practical applications, one possible bias error could be hidden in the charger efficiency curve as in the unipolar charging theories the specific dielectric constant is one parameter[84]. Though it has been found that there is some difference in the charger calibration curves with DOS and diesel soot, the origin could not be linked to difference in dielectric constant[85]. Another source of possible bias error is the existence of double charged particles. As in the DMA-impactor measurements of diesel soot it has customary to correct the effect of double charged particles, it should be verified that no such bias errors exist in the calibration. For demonstrative purposes following simulation was performed: ELPI is calibrated by measuring DMA classified unit density particles at the CMD of a range of log-normal distributions with geometric standard deviation (GSD) of 1.3. In the simulation particles up to three charges are exiting the DMA. However, when calculating the collection efficiency curves, only singly charged particles are assumed to exit the DMA. This approach leads to errors presented in Figure 9. Though the 50% collection efficiency diameter is correct with reasonable accuracy, there is some discrepancy at the low collection efficiencies of each stage. The charger efficiency curve is subjected to similar error though with the same simulation the maximum error is only 2% for the charger efficiency curve (Efficiency calculated from current ratio).
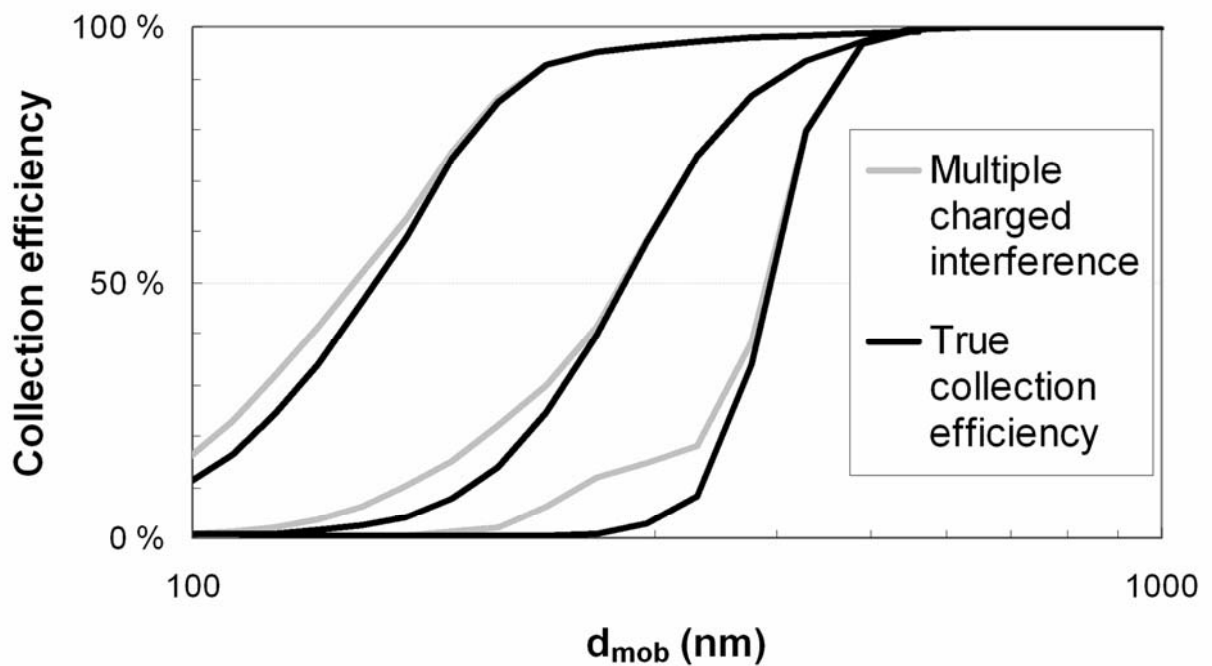
Figure 9 Collection efficiency curves obtained from calibration, if lognormal distributions with GSD 1.3 are used for calibration without taking multiple charged particles into account.

5 Mass transfer and effective density

The imbalance between vapour pressures at the surface of aerosol particle and surrounding gas phase results in mass transfer. At saturation ratios below unity, few molecular layers can be formed by adsorption[86]. When the saturation ratio exceeds unity condensation occurs. For condensation, several, slightly different equations have been proposed for the transition region where kinetic and continuum region theories are combined. However, as the theories are based on assumption of spherical particles, some simplifications from the real life have to be made. E.g. for diesel exhaust particles that seldom have spherical shape, the Kelvin effect is likely to differ from the theory.

Mass transfer changes the properties of the aerosol particles. One affected property of diesel exhaust particles is the effective density (Equation 16). As the effective density can be calculated from the mass and mobility equivalent particle diameter (Equation 14), simple model for changes in the effective density can be constructed based on changes in these two parameters. Assuming that large hydrocarbon (C28, with diameter of ~1nm, $\rho=0.8$g/cm^3), is adsorbed on a 18nm soot particle so that the surface area of the particle is covered with the hydrocarbon molecules, the effective density of the 18nm particle is decreased from 1.8g/cm^3 to 1.4g/cm^3 (Figure 10) while the diameter increases to 20nm. If the increase in the mobility diameter of the larger, non-spherical, agglomerate is assumed to be also 2nm, the effective density is increased due to the larger surface area (Figure 10). Additionally, it should be noted, that the spherical shape assumed for the hydrocarbon may be incorrect. As the C-C bond has already a length of 0.15nm, a C28 alkane could be over 4nm in length. Such a chain on the surface of a soot particle could have an effect on the mobility and effective density. Therefore, an adsorption layer could explain why reported effective densities for 10-20 nm soot particles are usually below 1.8g/cm^3.
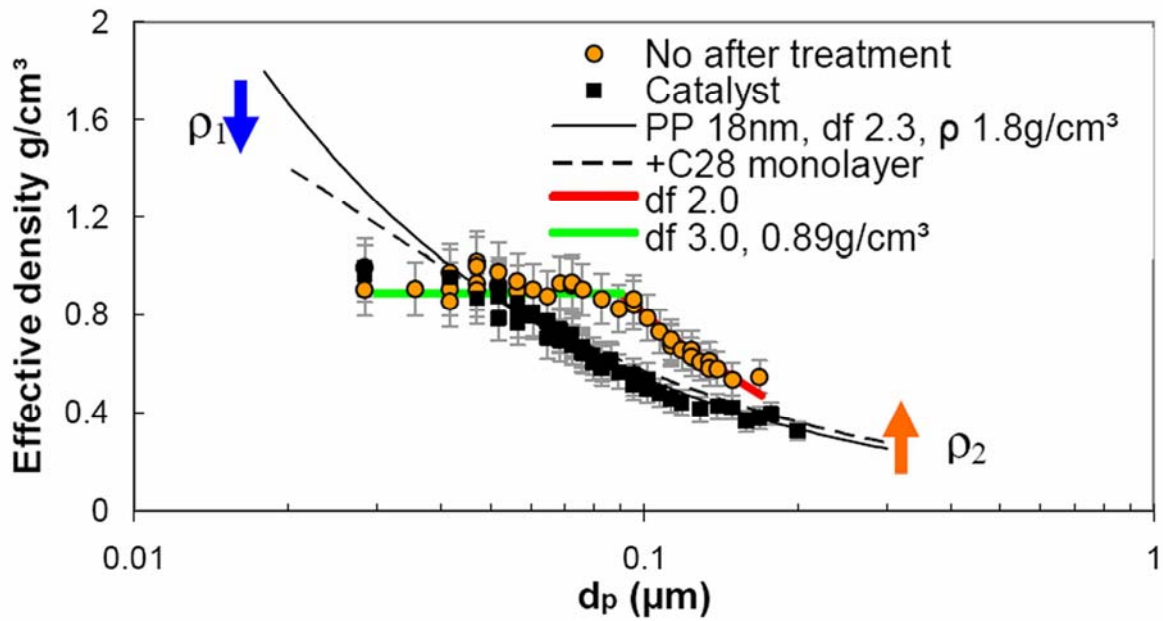
Figure 10 The effect of adsorbed (C28) hydrocarbon monolayer on the effective density of the diesel soot particle together with the measured effective densities with and without after treatment. Heavy-duty diesel engine. (Paper VI)

From Figure 10 it can also be seen that the difference in the measured effective densities with and without oxidation catalyst cannot be explained with simple adsorption model. Instead, as the decrease in the fractal dimension above 100nm is in line with the Equation 16, condensation might be the prevailing phenomena

5.1 Tandem DMA-ELPI method

Mass transfer studies have been conducted with e.g. Millikan cell. This setup has been widely used[50] for measuring substance properties such as diffusion coefficient[87,88], saturation vapour pressure[89] and surface tension[90], related to mass transfer. Another instrument setup used to study particle growth[91] or evaporation[92] is Tandem-DMA system[93,94]. In the TDMA particle diameters are measured with and without some sort of conditioning (Figure 11). From the

differences in particle diameters the mass change can be calculated. However, with particles that have voids, it could be possible that particle mass is increased without change in mobility. Therefore, by introducing e.g. the APM or an impactor into the TDMA setup, mass and its change can be measured also for non-spherical particles[95] (Paper V).

When an impactor is introduced into the TDMA system the particle mass and mass changes can be determined as a function of particle size (Paper V). The introduction of an impactor to the TDMA is not novel: an impactor has been installed after[69] and parallel[96] to the 2nd DMA. However, as the parallel ELPI-SMPS method presented in paper III can be applied to the TDMA setup (Figure 11), the advantages of TDMA can also be utilised with the same calculation method.

The TDMA-ELPI setup can be divided into two parts (Figure 11), aerosol conditioning and detection sections. The conditioning section consists of aerosol source, 1st DMA and aerosol conditioner. The detection section consists of parallel setup of ELPI and SMPS (or 2nd DMA). This division enables the use of the same calculation procedure as with normal parallel setup (Paper III) but utilizes the good resolution of the DMA/SMPS and without the limitations for the shape of the effective density as a function of particle size.
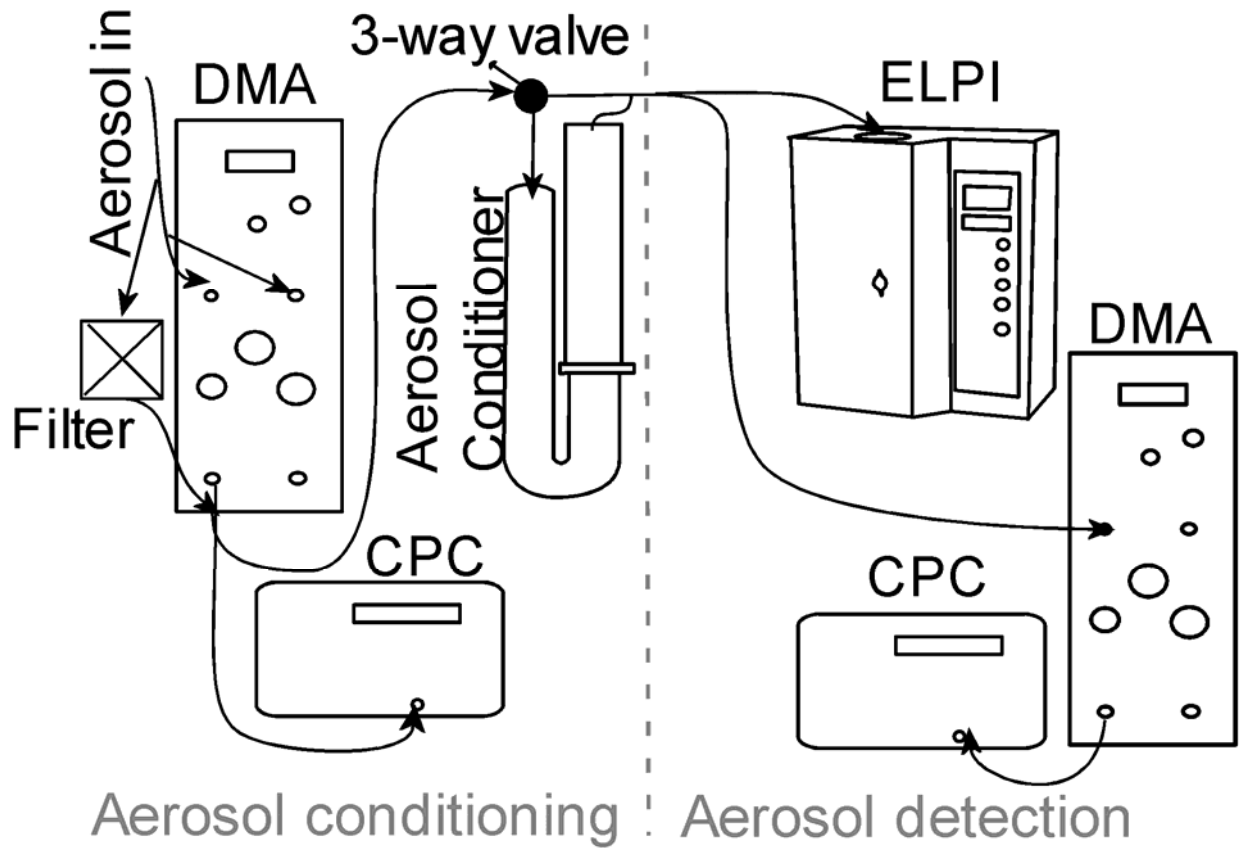
Figure 11 Basic setup of the TDMA-ELPI method. System can also be considered as aerosol conditioning and detection sections. (Paper V)

5.1.1 Performance of the TDMA-ELPI method

The use of the superior resolution of the DMA together with an impactor enables determination of the particle mass (Equation 13). Mass is suitable parameter for calculation with DMA-impactor systems as errors in the DMA classified size and effective density are partly cancelled in the impactor: I.e. if the monodisperse particles are measured larger than true diameter the calculation gives lower effective density for the particles. As a result 2% error in the mobility diameter results in 6% error already in the volume but only ~4% error in mass. The case holds even when the ELPI currents are subjected to noise. If 2% RMS noise is assumed for the measured mobility diameter,

together with 10% RMS noise for each channel of ELPI, 6% standard deviation for the particle mass is obtained.

The good resolution for particle mass can be utilised in measurement of mass change of particles. Based on the sensitivity analysis in paper V, ~17% mass change is detected with ~95% confidence limits when the particles are in the aerodynamic measurement range of ELPI. The smallest detection limit is defined by the collection efficiency of ELPI's lowest stage. This can be estimated to be in ideal case as low as 10^{-19}g for particles with high density. Unfortunately, it is unlikely that such a resolution is attainable in practice.

The performance of the TDMA-ELPI concept was also tested in laboratory. Spark generated, non-spherical silver particles were collapsed in a tube furnace servicing as an aerosol conditioner of the TDMA-ELPI setup. The structure of silver particles collapsed in the tube furnace providing more compact particles having the same mass. The mass of the particles were measured before and after the collapse. Results, presented in Figure 12, agreed well with the simulation as the measured mass change was within 18%.
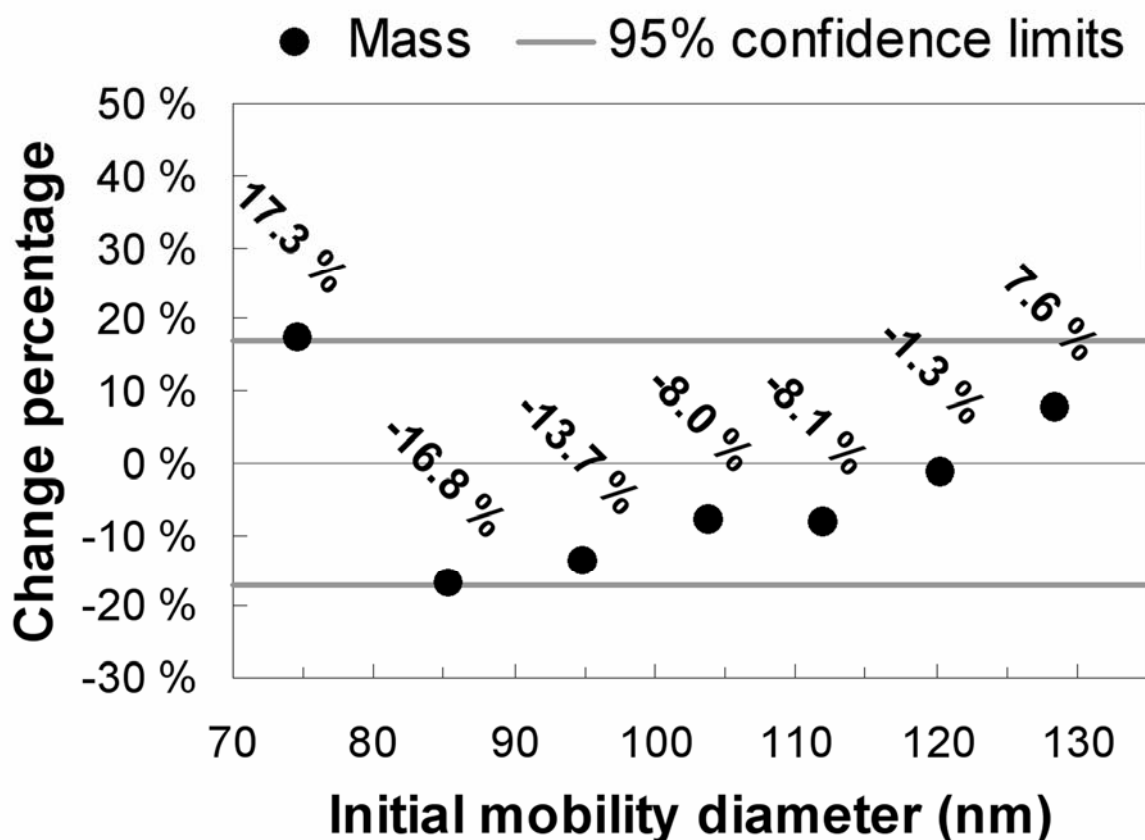
Figure 12 The measured mass change of silver particles in collapse experiment. (Paper V)

5.2 Application of mass change measurement

Compared to the normal TDMA measurement, the impactor enabled mass measurement allows detection of mass change also for non-spherical particles, which can have voids that hide the transferring matter. Examples of hidden mass can be found e.g. in diesel exhaust measurements where thermal treatment of particles with thermodenuder decreased the effective density but not the mobility[97]. In such case mass change may not be detected in normal TDMA measurement as there is no or negligible change in the particle mobility

diameter (Figure 13). In such case mass transfer can be detected by monitoring the particle effective density or mass.
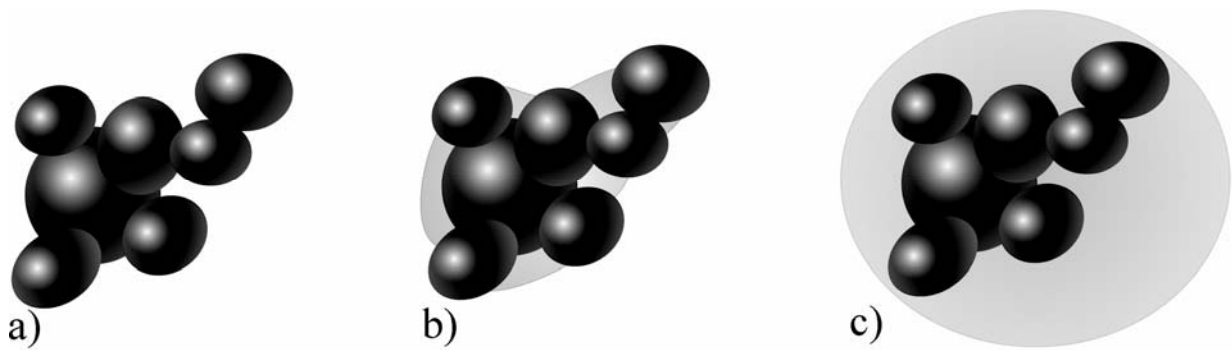

Figure 13 Schematic presentation of condensation on non-spherical particle. Negligible or no change in the mobility is observed until the voids of the particle are filled. Between a) and b) there could be change only in the effective density and mass, whereas in c) also the mobility diameter is significantly increased. (Paper V)

The TDMA-ELPI method enables accurate determination of mass making it suitable for the determination of the amount of mass transfer in the aerosol conditioner. When the mass change of particles has been determined as a function of particle size, the measurement points can be compared to mass transfer theories in order to get information of the process responsible of the mass change.

At the latest, when the voids of the particles have been filled particles start to grow in diameter. As the flux of mass to a particle is a function of the diameter, particles of different size have different growth rates on diameter axis. Though larger particles have larger flux of matter on it, the small particles grow relatively faster than the larger ones and the distribution gets narrower[98]. The

particle growth affects the shape of the mass change – core particle diameter curve (Figure 14).
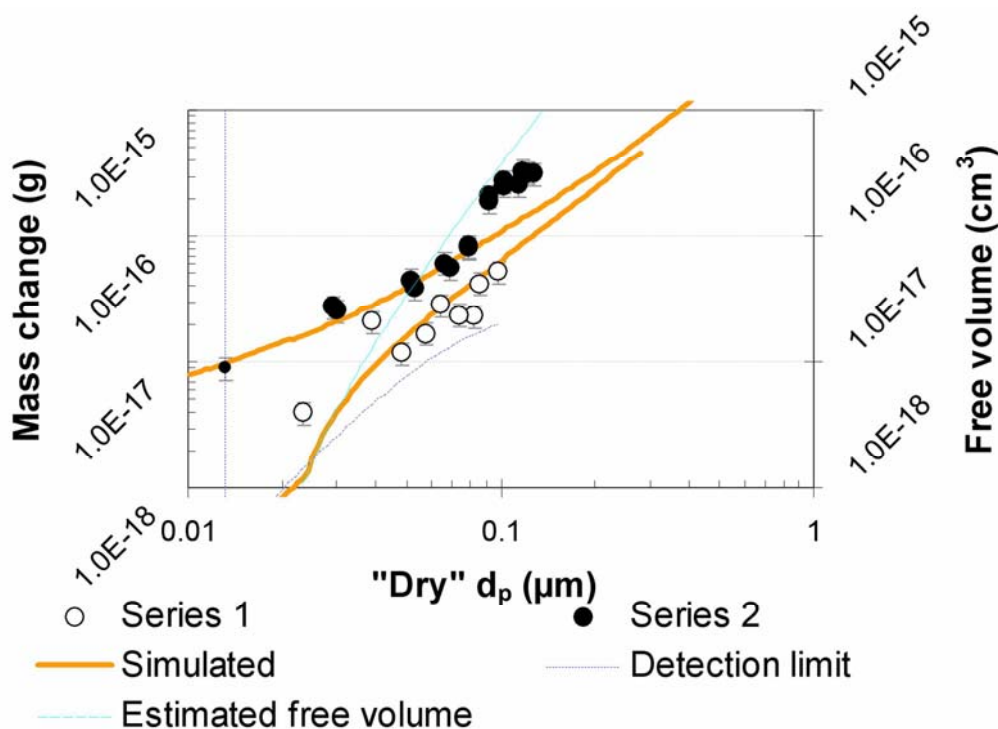

Figure 14 The measured mass change of two diesel exhaust measurement series and comparison to simulated mass change curves. The solid core diameter as x-axis. Simulated curves assume adsorption and condensation of C28 hydrocarbon on diesel soot particles. Condensation dominated mass transfer can be used to explain the measured mass change. Upper limit for free volume approximated from mobility diameter and mass (Secondary y-axis). (Paper VI)

When the mass transfer curve has been found it can be extrapolated to estimate the amount of substance in the particulate phase as a function of particle diameter. This enables the separation of the core and volatile mass distributions as can be done with e.g. TDMA-APM[99].

5.2.1 Density of condensed matter and TDMA-ELPI

The mass change measurements can be used to determine the density of the condensing matter directly from the particulate phase if two requirements are filled (Paper V): 1) At least one of the un- or conditioned particles has to be spherical. 2) The bulk density of the non-spherical particle is known or can be estimated.

To test the performance of the TDMA-ELPI setup in this case, laboratory measurements were performed with DOS coated, tube furnace generated silver particles (Paper V). As a result, the average density value (1.04 g/cm^3) for the condensed DOS agreed rather well with the bulk value (0.912g/cm^3) as presented in Figure 15.
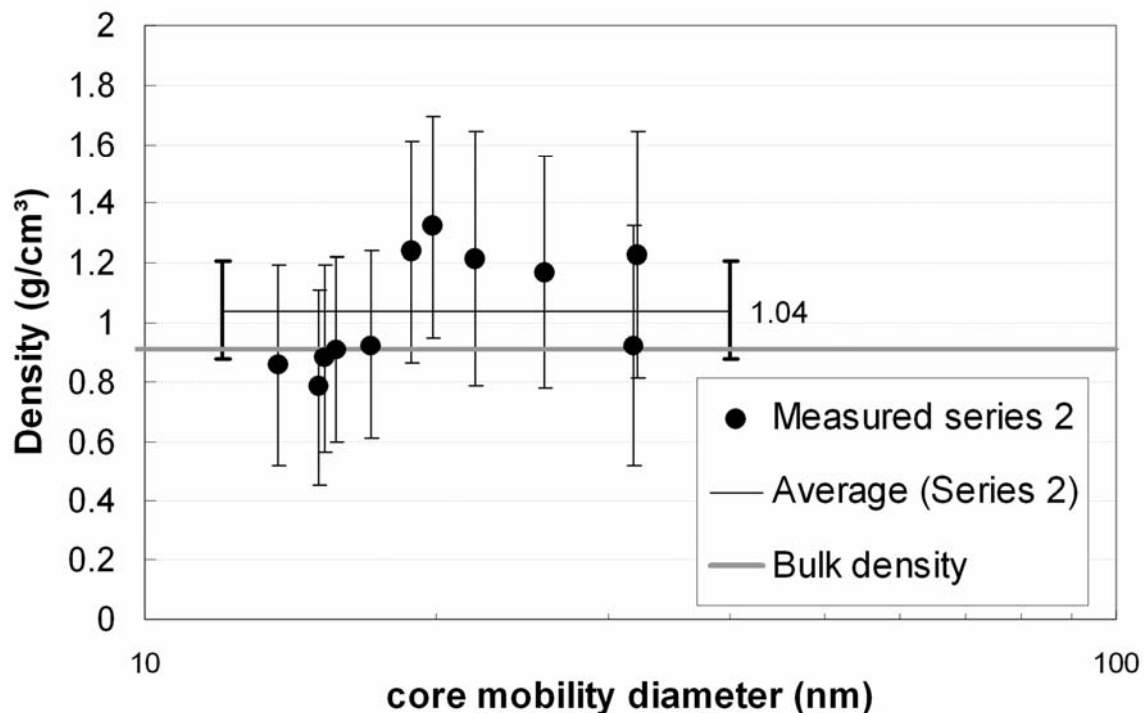
Figure 15 The obtained density for DOS when measured from DOS coated silver particle core. (Paper V)

The measurement of DOS density from coated silver particles was found to be very sensitive to temperature changes in the DOS condenser temperature. Difficulty in the measurement was that as the condensation starts to increase the diameter on the silver core particle the aerodynamic diameter starts to decrease. This means that the drag of the particles is increased more than the mass and therefore the particles end up in the lower stages in the impactor. This may lead to particle bounce in the impactor, which in turn leads to underestimation of particle mass.

The density of the condensed matter on diesel exhaust particles was also measured with heavy duty diesel engine (Paper VI). The density result, presented in Figure 16, agreed to previous studies suggesting densities close to lubricating oil or C28 [100]. The density was calculated for the series 2 of Figure 14 where particle growth was observed and particles could be assumed to be spherical. As the small particles grow faster than larger ones, they get spherical earlier during the condensation and fulfil the requirement 1 for the condensed density measurement. When particles have not yet become spherical, but slightly increased in diameter the volume of the condensed matter is overestimated. This overestimation leads to underestimation of volatile matter density as seen for the larger particles in Figure 16.
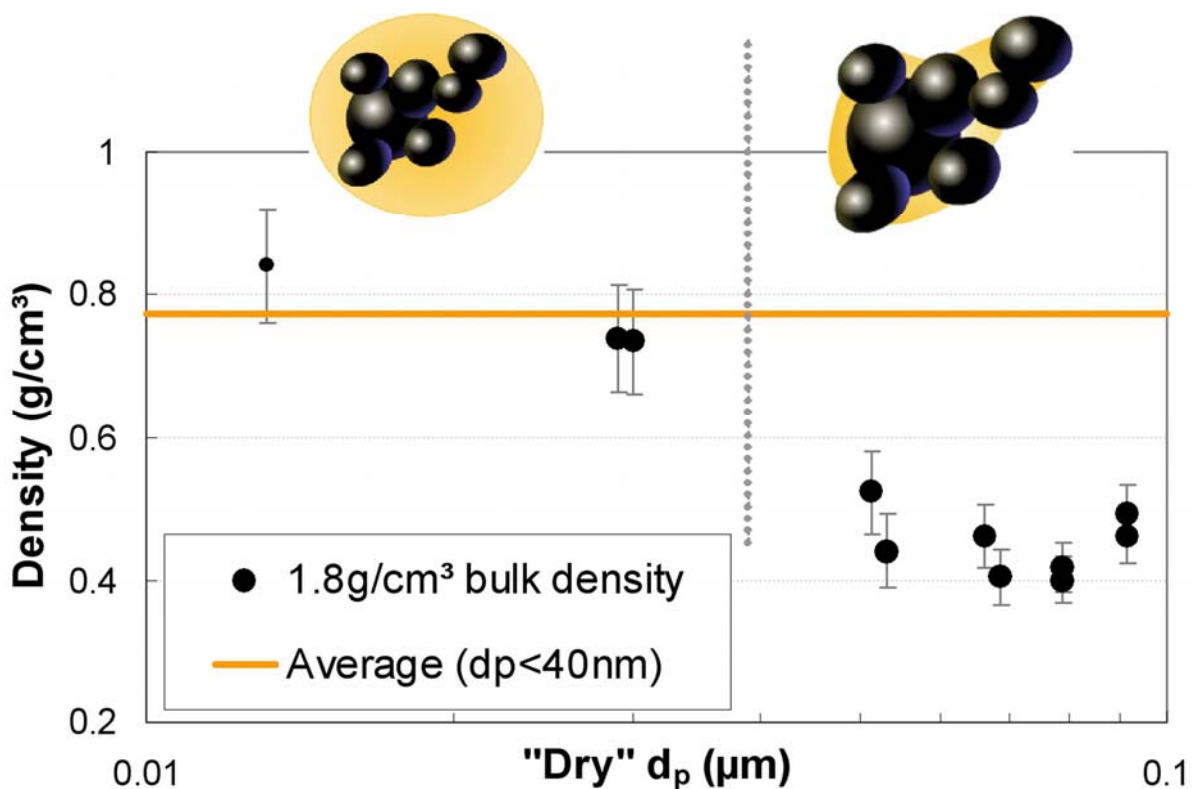
Figure 16 The measured density of volatile matter from the diesel exhaust particles. Calculated from the series 2 of Figure 14. If particles have not become spherical, the volatile matter density will be underestimated ($d_p > 40nm$). Small marker refer to point at the detection limit.

6 Performance comparison of ELPI-SMPS and TDMA-ELPI methods

In this chapter few simulations are made in order to demonstrate the performance differences between the ELPI-SMPS and TDMA-ELPI methods. The goal is to demonstrate how the condensation affects the results of the TDMA-ELPI and 2-parameter ELPI-SMPS methods. In all simulations ideal operation of both instruments without noise is assumed.

In the first simulation a diesel like particulate distribution is subjected to slight condensation and difference in the response of normal parallel ELPI–SMPS measurement system is considered. The input effective density profiles, case 1 (without condensation) and case 2 (with condensation), together with the obtained results (Fit) are presented in Figure 17. It can be seen from Figure 17 that slight condensation results in only small change in the result. Note that the fractal dimension, obtained from the ELPI-SMPS method is increased in this case, indicating mass increase of the particles.
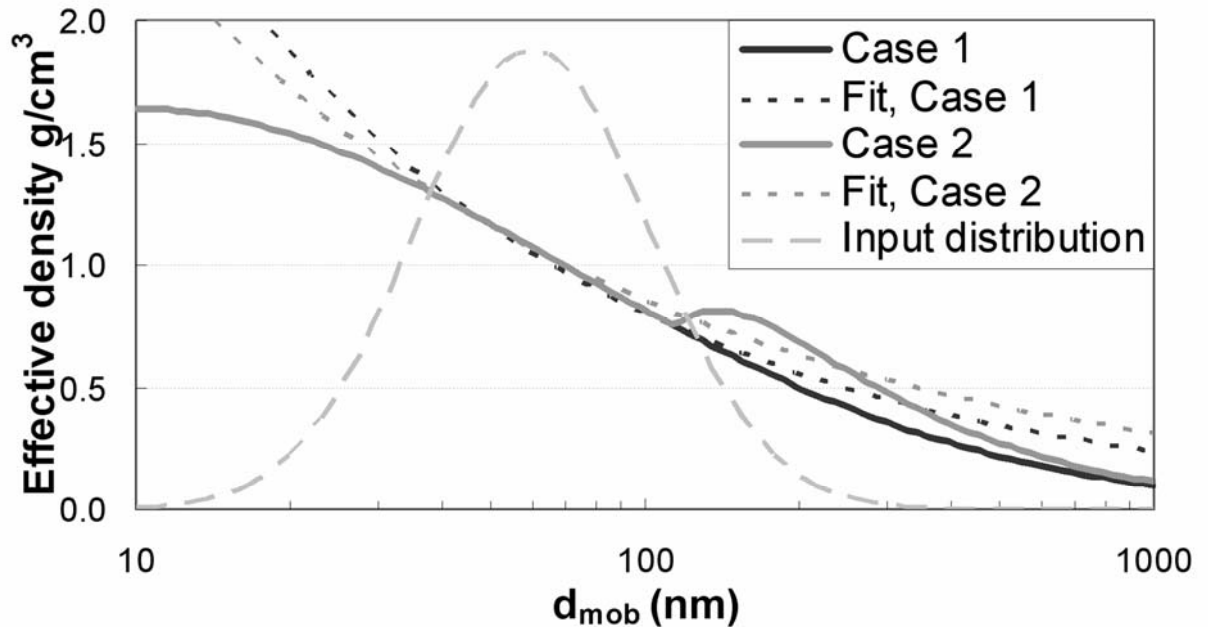
Figure 17 Simulation of detection of condensation from parallel ELPI-SMPS measurements. Input density profile from Figure 6 added with condensation. Comparison of the results (Fit) obtained with ELPI-SMPS method with (Case 2) and without (Case 1) condensation. The dashed line in the background shows the location and width of the diesel like number distribution used as input.

In a case of heavy condensation (case 3), when a particle growth occurs, more radical changes in the effective density profile may occur. In Figure 18 the

distribution presented in Figure 6 and Figure 17 is subjected to condensation of series 2 presented in Figure 14. Changes can be seen already in the shape of number distribution and significant drop of effective density is observed at small diameters. The shape of the true effective density is not very similar to the 2 parameter model though the effective density at the CMD is quite close to the true value.
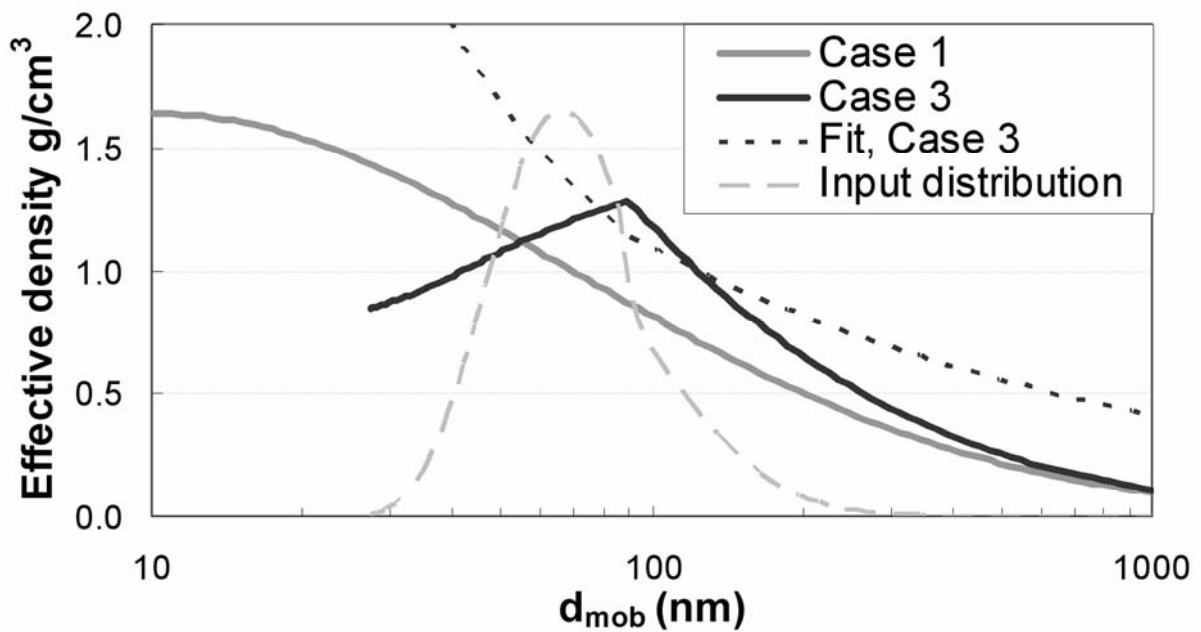

Figure 18 Simulation on effect of heavy condensation to parallel ELPI-SMPS density measurement. Input dry density profile from Figure 6 added with condensation of series 2 from Figure 14. The simulation result for number distribution plotted with dashed line in the background to visualise changes in the shape of the distribution.

Though the parallel ELPI-SMPS method is unable to find the correct effective density in the case of Figure 18, the method gives right indication for the mass change in the cases in figures 17 and 18. Therefore the parallel ELPI-SMPS method can be used to indicate the changes in aerosol mass.

The resolution of the parallel method is limited by the number of impactor stages that collect particles aerodynamically. Though in cases III and IV the amount of information is limited by the assumptions in density profile, it could be useful in some cases not to make any assumptions for the effective density.

In practice, it is possible to construct an algorithm where no assumptions for the effective density profile are needed with the ELPI-SMPS method. For example by connecting the effective density of consequent SMPS mobility diameter bins together and using and e.g. a genetic algorithm (GA) to minimise the difference between the simulated and measured ELPI currents no assumptions have to be made for the effective density profile. This approach finds the effective density in the vicinity of the mobility CMD as the methods presented in papers III and IV. In Figure 19 a simulation results with this approach to the condensation cases of figures 17 and 18 together with comparison to the TDMA-ELPI method is presented. In an ideal case, this method could bring some additional information about the shape of the effective density profile. In practice measurement noise is likely to ruin the sensitivity far away from the CMD.
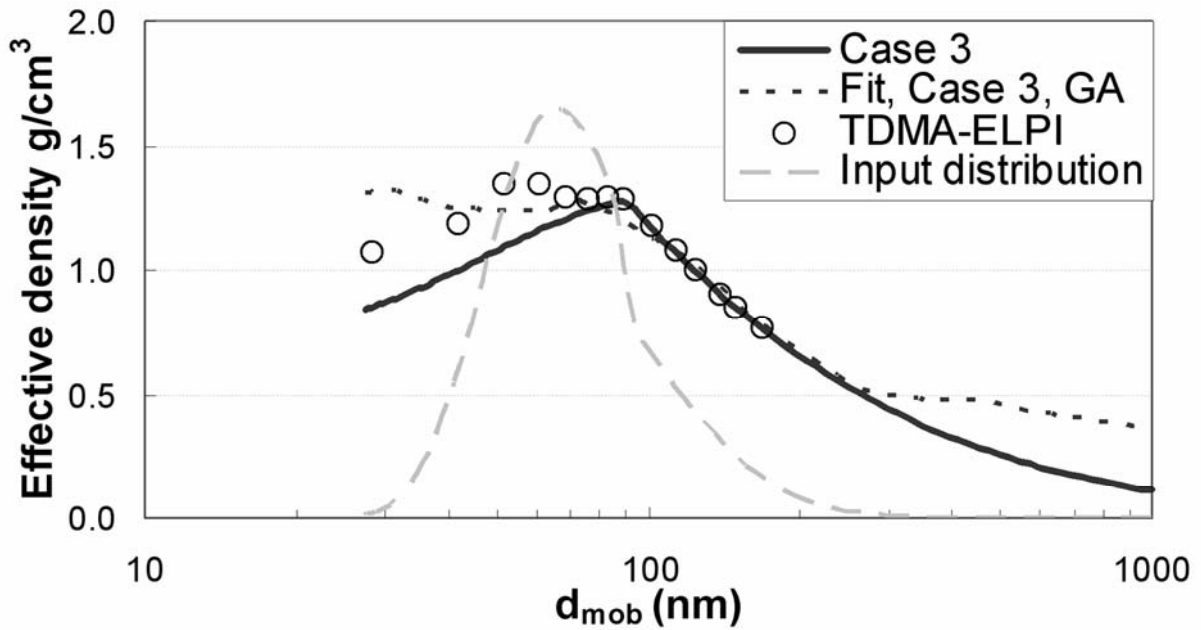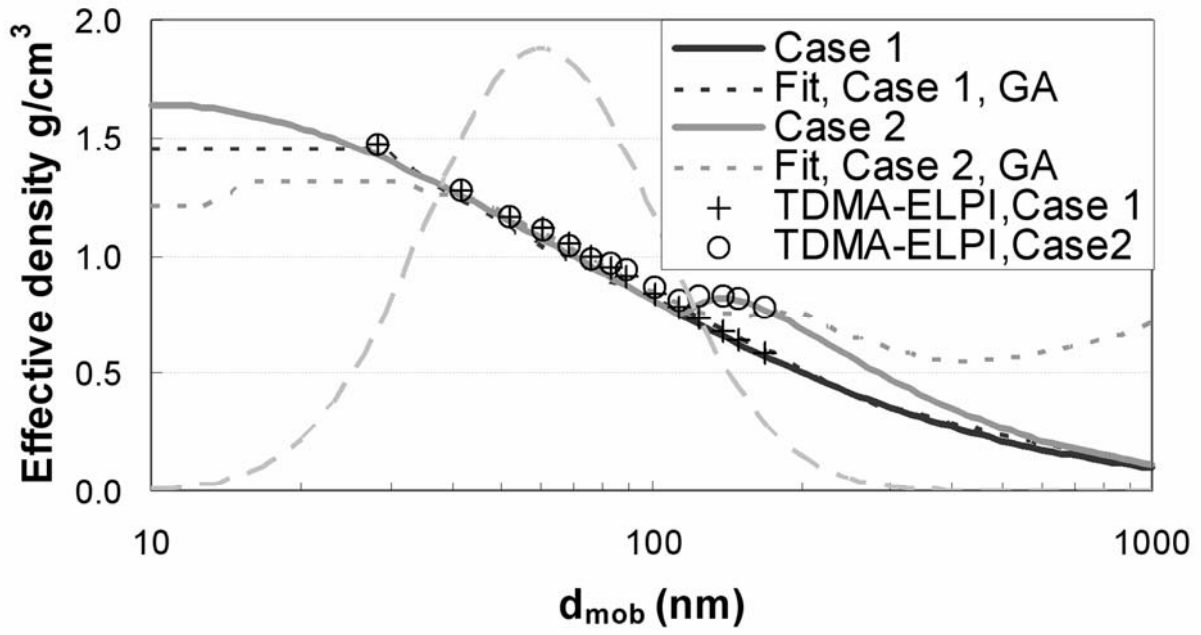
Figure 19 Input effective densities and the results obtained with the ELPI-SMPS using genetic algorithm and TDMA-ELPI method in different cases. a) Presenting results with no (case 1) or slight condensation (case2). b) Presenting results with heavy condensation (case 3). The dashed line in the background shows the location and width of the diesel like number distribution used as input.

7 Summary and conclusions

Accurate, representative and reproducible measurement information is needed in many research areas. In aerosol research the acquirement of experimental information starts with taking a sample. This initial step can already strongly affect the composition of sampled aerosol particles. Therefore it is necessary to realise, how the characteristics of the particles are changed during sampling and dilution. Additionally, it is important to know if the instrument response is affected by the changes in the particle composition or other parameters. Fortunately, no sign of evaporation of the nucleation mode particles were observed when the sub-zero sample was measured with instruments located at room temperature. This finding suggests that the instruments can be located at normal room temperature even when sub-zero exhaust sample is being measured.

As the effective density calculation method presented in paper III is being employed by other research groups, this thesis tries to help understanding of the possibilities and restrictions of the parallel ELPI-SMPS method and its application in the TDMA system, presented in paper V. However, it should be noted that most of the simulations were conducted with distributions having lognormal shape. With other kind of distributions and externally mixed aerosols the interpretation of the results may become more complex.

The simulations and laboratory experiments suggest that ELPI-SMPS and TDMA-ELPI methods are both suitable for determining the effective density of particles. Whereas the ELPI-SMPS method is practically suitable only for determination of the effective density or its profile in the vicinity of the CMD,

the TDMA-ELPI method enables determination of particle mass and possible mass transfer. As the measured mass change of particles in the TDMA-system could be explained with mass transfer theories, the separation of volatile and solid mass distributions is possible by inter-/extrapolating the theoretical curve fitted to the measurement results.

The recent advances in the real time mobility distribution measurement, such as fast mobility particle sizer (FMPS), enable the measurement of effective density in real time with the technique presented in papers III and IV. In addition, the method presented in paper III can be used to estimate the average densities for each mode of multi-modal size distributions in outdoor measurements[39].

References

[1] Stern A. C., Wohlers H. C., Boubel R. W., Lowry W. P. (1973) Fundamentals of Air Pollution, Academic Press Inc. ISBN 0-12-666560-5

[2] Chambers L.A., edited by Stern A. C. (1976) Air Pollution, Academic Press Inc. ISBN 0-12-666601-6

[3] History of Air Pollution Control in Philadelphia, http://www.phila.gov/health/units/ams/History.pdf obtained 8.11.2005

[4] Cooper D.C., Alley F.C. (1986) Air Pollution Control: A Design Approach. PWS publishers ISBN 0-534-059-104

[5] Haagen-Smit A.J., Wayne L.G., edited by Stern A. C. (1976) Air Pollution, Academic Press Inc. ISBN 0-12-666601-6

[6] Transportation Air Quality – Selected Facts and Figures US department of transportation, Federal Highway Administration, http://www.fhwa.dot.gov/environment/aqfactbk/factbk12.htm obtained 4.11.2005

[7] http://www.arb.ca.gov/html/brochure/history.htm 33 Fed. Reg. 8304 8305 (June 4, 1968)

[8] Chase R.E., Duszkiewicz G.J., Richert J.F.O., Lewis D., Maricq M.M., Xu N. (2004) PM Measurement Artifact: Organic vapour deposition on different filter media. *SAE paper* 2004-01-0967

[9] Brunekreef B., Holgate S.T. (2002) Air pollution and health. *The Lancet*, 360 19 1233-1242

[10] EPA report: Review of the national ambient air quality standards for particulate matter: Policy assessment of scientific and technical information http://www.epa.gov/ttn/oarpg/t1/reports/pmspch13.pdf obtained 2.11.2005

[11] Firket J. (1931) Sur les causes des accidents survenus dans la vallée de la Meuse, lors des brouillards de décembre 1930: résultats de l'expertise judiciaire faite par MM Dehalu, Schoofs, Mage, Batta, Bovy et Firket. Bull Acad R Méd Belg 1931; 11: 683-734 cited in Nemery B., Hoet P., Nemmar A. (2001) The Meuse Valley fog of 1930: an air pollution disaster, *The Lancet* 357 3:704-708

[12] Nemery B., Hoet P., Nemmar A. (2001) The Meuse Valley fog of 1930: an air pollution disaster, *The Lancet* 357 3:704-708

[13] Health Aspects of air Pollution – Results from the WHO project "systematic review of health aspects of air pollution in Europe" June 2004 http://www.euro.who.int/document/E83080.pdf obtained 11.11.2005

[14] Fine Particle (PM2.5) Designations http://www.epa.gov/pmdesignations/documents/Sep05/factsheet.htm obtained 2.11.2005

[15] Proposal for a directive of the European parliament and the council on ambient air quality and cleaner air for Europe (presented by the commission), COM(2005)447, 2005/0183(COD)/{SEC(2005)1133}

[16] Goo J., Kim C. (2003) Theoretical analysis of particle deposition in human lungs considering stochastic variations of airway morphology, *Journal of Aerosol Science* 34 585-602

[17] Health Aspects of Air Pollution – Answers to follow-up questions from CAFÉ, Report on a WHO working group meeting, Bonn, Germany 15-16 January 2004 ; http://www.euro.who.int/document/E82790.pdf obtained 11.11.2005.

[18] Shimpi S. (2003) EPA Clean Diesel Engine Implementation Workshop, August 2003 http://www.epa.gov/otaq/regs/hd2007/wrkshop2/shimpi.ppt obtained 10.1.2006

[19] Khalek I.A. (2005) 2007 Diesel particulate measurement research, Final report, Project E-66-Phase 1, Coordinating research council. http://www.crcao.com/reports/recentstudies/final%20Rport-10415-Project%20E-66-Phase%201-R3.pdf

[20] Heywood J. B., (1988) Internal Combustion engine fundamentals. McGraw-Hill Book Company. ISBN 0-07-100499-8

[21] Smith O. (1981) Fundamentals of soot formation in flames with application to diesel engine particulate emissions. *Prog. Energy Combustion Science* 7 275-291

[22] Kittelson D.B. (1998) Engines and nanoparticles: A review. *Journal of Aerosol Science* 29 5/6:575-588

[23] Abdul-Khalek I., Kittelson D., Brear F. (1999) The influence of dilution conditions on diesel exhaust particle size distribution measurements. *SAE Technocal Paper Series* 1999-01-1142

[24] Khalek I.A., Kittelson D.B., Brear F. (2000) Nanoparticle growth during dilution and cooling of diesel exhaust: Experimental investigation and theoretical assessment. *SAE Technical Paper Series* 2000-01-0515

[25] Kerminen V.-M., Mäkelä T., Ojanen C., Hillamo R., Vilhunen J., Rantanen L., Havers N., Bohlen A., Klockow D. (1997) Characterization of the particulate phase in the exhaust from a diesel car. *Environmental Science & Technology* 31 7:1883-1889

[26] Ålander T., Leskinen A., Raunenmaa T. (2004) Characterization of diesel exhaust particles: Effect of fuel reformulation, exhaust aftertreatment, and engine operation on particle carbon composition and volatility. *Environmental Science & Technology* 38 9:2707-2714

[27] Lemmetty M., Pirjola L., Mäkelä J., Rönkkö T., Keskinen J. Computation of maximum rate of water-sulphuric acid nucleation in diesel exhaust. *Journal of aerosol Science* 37 11:1596-1604

[28] Mikkanen P., Moisio M., Keskinen J., Ristimäki J., Marjamäki M. (2001) Sampling method for particle measurement of vehicle exhaust. *SAE Technical Paper Series* 2001-01-0219

[29] Ning Z., Cheung C.S., Liu S.X. (2003) Experimental investigation of the effect of exhaust gas cooling on diesel particulate. *Journal of Aerosol Science* 35 3:333-345

[30] Maricq M., Chase R., Podsiadlik D., Vogt R. (1999) Vehicle exhaust particle size distribution: Comparison of tailpipe and dilution tunnel measurements. *SAE Technical Paper Series* 1999-01-1461

[31] Vaaraslahti K., Keskinen J., Giechaskiel B., Solla A., Murtonen T., Vesala H. (2005) Effect of lubricant on the formation of heavy duty diesel exhaust nanoparticles. *Environmental Science & Technology* 39 21:8497-8504

[32] Ntziachristos L., Giechaskiel B., Pistikopoulos P., Samaras Z., Mathis U., Mohr M., Ristimäki J., Mohr M., Ristimäki J., Keskinen J., Mikkanen P., Casati R., Scheer V., Vogt R. (2004) Performance evaluation of a novel sampling and measurement system for diesel exhaust particle characterization. *SAE Technical Paper Series* 2004-01-1439

[33] Knutson E.O., Whitby K.T. (1975) Aerosol classification by electric mobility: Apparatus, theory, and application. *Journal of Aerosol Science* 6:443-451

[34] Zhang S-H., Akutsu Y., Russell L.M., Flagan R.C., Seinfeld J.H. (1995) Radial differential mobility analyzer. *Aerosol Science and Technology* 23 357-372

[35] Mohr M., Lehmann U., Rütter J. (2005) Comparison of mass-based and non-mass-based particle measurement systems for ultra-low emissions from automotive sources. *Environmental Science & Technology* 39 7:2229-2238

[36] Agarwal J.K., Sem G.J. (1980) Continuous flow, single-particle-counting condensation nucleus counter. *Journal of Aerosol Science* 11 4:343-357

[37] Dilara P., Andersson J. (2005) Report on first results from LD interlab. Working paper No. GRPE-PMP-15-2 15th PMP working meeting Geneva 31st May 2005 http://www.unece.org/trans/doc/2005/wp29grpe/PMP-2005-12-02e.pdf Obtained 11.1.2005

38 Morawska L., Thomas S., Bofinger N., Wainwright D., Neale D. (1998) Comprehensive Characterization of Aerosols in a Subtropical Urban Atmosphere: Particle Size Distribution and Correlation with Gaseous Pollutants, *Atmospheric Environment* 32 2467-2478

39 Virtanen A., Rönkkö T., Kannosto J., Ristimäki J., Mäkelä J., Keskinen J., Pakkanen T., Hillamo R., Pirjola L., Hämeri K. (2006) Winter and summer time size distributions and densities of traffic-related aerosol particles at a busy highway in Helsinki. *Atmospheric Chemistry and Physics* 2411-2421

40 Milestones in Auto Emission Control. US Environmental Protection Agency, Office of Mobile Sources, EPA 400-F-92-014 http://www.epa.gov/otaq/consumer/12-miles.pdf obtained 12.1.2006

[41] Directive 2001/100/EC, Offical Journal of European Communities 18.1.2002 http://www.europa.eu.int/eur-lex/pri/en/oj/dat/2002/l_016/l_01620020118en00320034.pdf

[42] Keskinen J., Pietarinen K., Lehtimäki M. (1992) Electrical Low Pressure Impactor. *Journal of Aerosol Science* 23:353-360

[43] Marjamäki M. (2003) Electrical Low Pressure Impactor: Modifications and Particle Collection Characteristics Ph.D. Thesis Tampere University of Technology, ISBN 952-15-1111-7

[44] Wang S.C., Flagan R.C. (1990) Scanning Electrical Mobility Spectrometer, *Aerosol Science and Technology* 13:230-240

[45] Koike E., Hirano S., Furuyama A., Kobayashi T. (2004) cDNA microarray analysis of rat alveolar epithelial cells following exposure to organic extract of diesel exhaust particles. *Toxicology and Applied Pharmacology* 201 2:178-185

[46] Koike E., Kobayashi T. (2005) Organic extract of diesel exhaust particles stimulates expression of Ia and costimulatory molecules associated with antigen presentation in rat peripheral blood monocytes but not in alveolar macrophages. *Toxicology and Applied Pharmacology* 209 3:277-285

[47] Mayer A., Czerwinski J., Scheidegger P. (1996) Trapping efficiency depending on particulate size. *SAE Technical Paper Series* 960472

[48] Lüders H., Krüger M., Stommel P., Lüers B. (1998) The role of sampling conditions in particle size distribution measurements. *SAE Technical Paper Series* 981374

[49] Vaaraslahti K., Virtanen A., Ristimäki J., Keskinen J. (2004) Nucleation mode formation in heavy-duty diesel exhaust with and without a particulate filter. *Environmental Science & Technology* 38 18:4884-4890

[50] Davis J.E., edited by Willeke K. and Baron P.A. (1993) Aerosol Measurement. Van Nostrand Reinhold ISBN 0-442-00486-9

[51] Ehara K., Hagwood C., Coackley K.J. (1996) Novel method to classify particles according to their mass to charge ratio – Aerosol particle mass analyzer. *Journal of Aerosol Science* 27 2:217-234

[52] Bronec E., Renoux A., Boulaud D., Pourprix M. (1999) Effect of gravity in differential mobility analysers. A new method to determine the density and mass of aerosol particles. *Journal of Aerosol Science* 30 1:89-103

[53] Williams K., Fairchild C., Jaklevic J., edited by Willeke K. and Baron P.A. (1993) Aerosol Measurement. Van Nostrand Reinhold ISBN 0-442-00486-9

[54] Eatough D., Long R., Modey W., Eatough N. (2003) Semi-volatile secondary organic aerosol in urban atmospheres: meeting a measurement challenge. *Atmospheric Environment* 37 1277-1292

[55] Moisio M., Niemelä V. (2002) Device for continuous measurement of density ond mass concentration of vehicle exhaust aerosol. 6th International Aerosol Conference IAC Taipei Taiwan. http://www..com/dmm.shtml Obtained 16.1.2006

[56] Lehmann U., Niemelä V., Mohr M. (2004) New method for time-resolved diesel engine exhaust particle mass measurement. *Environmental Science & Technology* 38 21:5704-5711

[57] Kasper G. (1982) Dynamics and Measurement of Smokes. I Size Characterization of nonspherical Particles, *Aerosol Science and Technology* 1:187-199

[58] Kelly W.P. McMurry P.H. (1992) Measurement of Particle density by Inertial Classification of Differential Mobility Analyser-Generated Monodisperse Aerosol, *Aerosol Science and Technology* 17:199-212

[59] Brockmann J.E., Rader D.J (1990) APS response to nonspherical particles and experimental determination of dynamic shape factor, *Aerosol Science and Technology* 13 2:162-172

[60] Rogak S. N., Flagan R., Nguyen H. (1993) The mobility and structure of aerosol agglomerates. *Aerosol Science and Technoloogy* 18:25:47

[61] Baron P., Sorensen C., Brockmann J. (2001) Nonspherical particle measurements: Shape factors, Fractals and Fibers. Aerosol Measurement: Principles, Techniques and Applications, 2nd edition, Edited by Paul A. Baron and Klaus Willeke. ISBN 0-471-35636-0.

[62] Witten T., Sander L. (1981) Diffusion limited aggregation, a kinetic critical phenomena. *Phys. Rev. Letters* 47 1400-1403

[63] Skillas G., Küntzel S., Burtscher H., Baltensperger U., Siegmann K. (1998) High fractal-like dimension of diesel soot agglomerates. *Journal of Aerosol Science* 29 4:411-419

[64] Park K., Kittelson D., Zachariah M., McMurry P. (2004) Measurement of Inherent Material Density of Nanoparticle Agglomerates. *Journal of Nanoparticle Research* 6 267-272

[65] Park K., Cao F., Kittelson D., McMurry P. (2003) Relationship between particle mass ans mobility for diesel exhaust particles. *Environmental Science & Technology* 37 3:577-583

[66] Hering S.V., Friedlander S.K., Collins J.J., Richards L.W. (1979), Design and Evaluation of a New Low-Pressure Impactor. *Environmental Science & Technology* 13:184-188

[67] Hillamo R., Kauppinen E. (1991) On the Performance of the Low Pressure Impactor. *Aerosol Science and Technology* 14:33-47

[68] Marple V.A., Rubow K. L., Behm S.M. (1991) A Microorfice Uniform Deposit Impactor (MOUDI): Description, Calibration, and Use. *Aerosol Science and Technology* 14:434-446

[69] Kütz S., Scmidt-Ott A. (1990) Use of a low-pressure impactor for fractal analysis of submicron particles. *Journal of Aerosol Science* 21 S1:S47-S50

[70] Hering S.V., Stolzenburg M.R. (1995) On-line determination of particle size and density in the nanometer size range. *Aerosol Science and Technology* 23:155-173

[71] Schleicher B., Künzel S., Burtscher H. (1995) In Situ Measurement of Size and Density of Submicron Aerosol Particles. *Journal of Applied Physics* 78:4416-4422

[72] Fernandez De La Mora F., Schmidt-Ott (1993) Performance of a hypersonic impactor with silver particles in the 2nm range. *Journal of Aerosol Science* 24 3:409-415

[73] Ahlvik P., Ntziachristos L., Keskinen J., Virtanen A. (1998) Real ime measurement of diesel particle size distribution with an electrical low pressure impactor. *SAE Technical Paper Series* 980410

[74] Maricq M.M., Podsiadlik D.H., Chase R.E. (2000) Size distribution of motor vehicle exhaust PM: A Comparison between ELPI and SMPS measurements. *Aerosol Science and Technology* 33:239-260

[75] Marjamäki M. (2003) Electrical low pressure impactor: Modifications and particle collection characteristics. Ph.D. Thesis, Figure 17 on page 45. ISBN 952-15-1111-7

[76] Marjamäki M., Keskinen J., Chen D.-R., Pui D.Y.H. (2000) Performance evaluation of the electrical low-pressure impactor (ELPI). *Journal of Aerosol Science* 31 2:249-261

[77] Marjamäki M. (2003) Electrical low pressure impactor: Modifications and particle collection characteristics. Ph.D. Thesis. ISBN 952-15-1111-7

[78] Maricq M., Xu N. (2004) The effective density and fractal dimension of soot particles from premixed flames and motor vehicle exhaust. *Journal of Aerosol Science* 35:1251-1274

[79] Virtanen A., Ristimäki J., Vaaraslahti K., Keskinen J. (2004) Effect of engine load on diesel soot particles. *Environmental Science & Technology* 38 9:2551-2556

[80] Keskinen J., Marjamäki M., Virtanen A., Mäkelä T., Hillamo R. (1999) Electrical calibration method for cascade impactors. *Journal of Aerosol Science* 30 1:111-116

[81] Marjamäki M., Lemmetty M., Keskinen J. (2005) ELPI response and data reduction I:Response functions. *Aerosol Science and Technology* 39 7:575-582

[82] Pak S.S., Liu B.Y.H., Rubow K.L. (1992) Effect of coating thickness on particle bounce in inertial impactors. *Aerosol Science and Technology* 16:141-150

[83] Reischl G.P., John W. (1978) The collection efficiency of impaction surfaces: A new impaction surface. Staub – Reinhalt. Luft 38 2:55

[84] Adachi M., Kousaka Y., Okuyama K. (1985) Unipolar and bipolar diffusion charging of ultrafine aerosol particles. *Journal of Aerosol Science* 16 2:109-123

[85] Ntziachristos L., Giechaskiel B., Ristimäki J., Keskinen J. (2004) Use of a corona charger for the characterisation of automotive exhaust aerosol. *Journal of Aerosol Science* 35 8:943-963

[86] Kittelson D. and Dolan D. (1980) Diesel exhaust aerosols, in: Generation of aerosols and facilities for exposure experiments. Edited by Willeke K.Ann arbor Science Publishers Inc. ISBN 0-250-40293-9

[87] Monchick L., Reiss H. (1954) Studies of evaporation of small drops. *Journal of chemical physics* 22 3:831-836

[88] Davis J.E., Ray A.K. (1977) Determination of diffusion coefficients by submicron droplet evaporation. *The journal of chemical physics* 67 2:414-419

[89] Ray A.K., Davis J., Ravindran P. (1979) Determination of ultra-low vapour pressures by submicron droplet evaporation. *The journal of chemical physics* 71 2:582-587

[90] Shereshefsky J.L., Steckler S. (1936) A study of the evaporation of small drops and of the relationship between surface tension and curvature. *Journal of chemical physics* 4:108-115

[91] Joutsensaari J., Toivonen T., Vaattovaara P. Vesterinen M., Vepsäläinen J., Laaksonen A. (2004) Time-resolved growth behavior of acid aerosols in ethanol vapor with tandem-DMA technique. *Journal of Aerosol Science* 35 7:851-867

[92] Bilde M., Pandis S. (2001) Evaporation rates and Vapour pressures of individual aerosol species formed in the atmospheric oxidation of α- and β-pinene. *Environmental Science & Technology* 35 16:3344-3349

[93] Liu B.Y.H., Pui D.Y.H., Whitby K.T., Kittelson D.B. Kousaka Y., McKenzie R.L (1978) The aerosol mobility cromatograph: A New detector for sulphuric acid aerosols. *Atmospheric Environment* 12:99-104

[94] Rader D.J., McMurry P.H. (1986) Application of the tandem differential mobility analyzer to studies of droplet growth or evaporation. *Journal of Aerosol Science* 17 5:771-787

[95] McMurry P.H., Wang X., Park K., Ehara K. (2002) The relationship between mass and mobility for atmospheric particles: A new technique for measuring particle density. *Aerosol Science and Technology* 36 2:227-238

[96] Seipenbusch M., Heel A., Weber A., Kasper G. (2002) Determination of coeating thickness of DEHS on submicron particles by means of low pressure impaction. *Chemical Engineering & Technology* 25 1:77-82

[97] Virtanen A. (2004) Physical characterization of diesel soot particles, Ph.D. Thesis. Tampere University of Technology. ISBN 952-15-1167-2

[98] Seinfeld J.H., Pandis S.N. (1998) Atmosheric chemistry and physics From air pollution to climate change. Figure 12.3 John Wiley & Sons ISBN 0-471-17816-0

[99] Sakurai H., Park K., McMurry P.H., Zarling D.D., Kittelson D.B., Ziemann P.J. (2003) Size-dependent mixing characteristics of volatile and non-volatile components in diesel exhaust aerosols. *Environmental Science & Technology* 37 24:5487-5495

[100] Sakurai H., Tobias H.J., Park K., Zarling D., Docherty S., Kittelson D.B., McMurry P.H., Ziemann P.J. (2003) On-line measurement of diesel nanoparticle composition and volatily. *Atmospheric Environment* 37 9-10:1199-1210

Tampereen teknillinen yliopisto
PL 527
33101 Tampere

Tampere University of Technology
P.O. Box 527
FIN-33101 Tampere, Finland